

Czech University of Life Sciences in Prague



Diploma Thesis

2013

Thi Thanh Huyen DAO

Czech University of Life Sciences in Prague
Faculty of Agrobiography, Food and Natural Resources
Department of Water Resources



**Evaporation from free water surface – measurement,
calculation and broader context**

Diploma Thesis

Author: Huyen Thi Thanh Dao

Supervisor: Ing. František Doležal, CSc.

© 2013 ČZU v Praze

Declaration

I hereby declare this M.Sc. thesis on “Evaporation from free water surface – measurement, calculation and broader context” is my independent work and effort, carried out under the guidance of my supervisor. All scientific literature and all other information sources used in it have been duly acknowledged in the text and in the list of references in the end of the thesis. As an author of the thesis I also declare that, in association with writing it, I did not infringe copyrights of third persons.

Prague,

Signature

Acknowledgement

Conducting a research and expressing its findings in a thesis have always been inspiring though stressful work. To have the results today, I would like to express my special thanks to Ing. CSc. František Doležal for his great patience, his useful advice, and for the freedom he gave to me when I conducted this thesis. I would like to thank Dr. Ing. Martin Možný for his consultations and his colleagues from the Czech hydrometeorological institute for assistance at maintenance of the EWM pan, Ing. Jaroslav Fišák from the Institute of atmospheric physics, Czech Academy of Sciences in Prague for providing meteorological data for my thesis and Mr. Getu Bekere Mekonnen for letting me use his data and read his manuscript.

I would also like to extend my gratitude to people I have met, my teachers, and my friends who inspired and instructed me a lot during my two years living in Prague.

Finally, to my beloved family who live far but always keep an eye on me, encourage me, and to my dearest friends Van, Hoai, Trang who are always eager to listen to me and help me unconditionally.

Evaporation from free water surface – measurement, calculation and broader context

Summary

This thesis aims to quantify the amount of water surface evaporation with special regard to the EWM evaporation pan and to relate the direct measurements to the Penman and other empirical equations. Based on the available 10-minute interval data on the EWM pan evaporation and the data on precipitation for the same intervals, the net water surface evaporation was estimated for the period from July 2010 to October 2012 (excluding the time EWM pan did not function in winter). From the processing data, UFA raingauge appeared to underestimate the actual precipitation on average 5:3 times, and malfunction when heavy rains occurred. Thus the net evaporation was estimated only from the fluctuation of water level in EWM pan.

Other available weather data, including the dry/wet bulb temperature, water surface temperature, air humidity, wind speed and short-wave solar radiation were also summarized and corrected. These data were then used as input for the Penman and other equations to obtain semi-empirical daily values of evaporation from water surface. All data were also related to the reference crop evapotranspiration according to the FAO 56 Penman-Monteith equation and the EWM pan coefficient were estimated. A comparison between the evaporation rates directly measured and those calculated by different methods shows that a new albedo value of 0.3486, when applied to summer time data, would improve the performance of the Penman equations. The pan coefficient $k_{\text{pan}} = 0.44$ was found as adequate for all-season estimation of the FAO 56 reference crop evapotranspiration from EWM pan data. The result of this study contributed to optimization of the EWM data processing methods and to the analysis of variation of water surface evaporation within the diurnal cycle, as well as over longer periods.

Keywords: potential evaporation, Penman, empirical equations, gross and net evaporation, diurnal variation, precipitation, EWM pan

List of contents

List of Figures and table	vi
1. Introduction	2
2. Scientific hypotheses and objectives of work	4
3. Literature Overview	5
3.1. Definitions	5
3.2. Units and scales:	6
3.3. Physical principles of evaporation.....	7
3.4. Measurements	9
3.5. Overview of previous researches.....	15
4. Materials and methods.....	19
4.1. Study area	19
4.2. Models	19
4.3. Measurements	19
4.3.1. Measurement of potential evaporation.....	19
4.3.2. Measurement of precipitation	22
4.3.3. Measurements of atmospheric variables	22
4.4. Basic data processing.....	24
4.4.1. Temperature	24
4.4.2. Vapor pressure	24
4.3.3. Solar radiation	26
4.3.4. Wind speed.....	27
4.4. Bridging gaps in data	27
4.4.1. Bridging wind speed	28
4.4.2. Bridging solar radiation	28
4.4.3. Bridging water temperature	28
4.4.4. Bridging wet-bulb temperature	29

4.4.5 Temperature examples	29
5. Results	33
5.1. Processing pan measurements	33
5.2. Dalton's equation for potential evaporation	45
5.3. Penman's equation for potential evaporation	47
5.4. FAO 56 Penman-Monteith equation for reference crop evapotranspiration	51
6. Discussion	53
7. Conclusion.....	56
Bibliography.....	57
Appendix	viii

List of Figures and table

Figure 1. Flux of water molecules over a water surface	9
Figure 2. EWM pan	20
Figure 3. Optical sensor of EWM pan.....	20
Figure 4. Tipping bucket raingauge	22
Figure 5. Pyranometer	23
Figure 6. Temperature comparison between two sources	30
Figure 7. Dry-bulb, wet-bulb and water surface temperature - 2011	31
Figure 8. Estimate Net evaporation on EWM pan measurement	34
Figure 9. The 3-hour evaporation rates	36
Figure 10. The 6-hour evaporation rates	36
Figure 11. Daily evaporation rates	37
Figure 12. Comparison between two ways of processing EWM pan measurement	40
Figure 13. Rough estimation of precipitation from EWM pan and UFA raingauge.....	41
Figure 14. The 6-hour evaporation rates - 2010.....	42
Figure 15. Diurnal variation of evaporation rate - 2010.....	43
Figure 16. Turbulent exchange function - 2011	46
Figure 17. Comparison of different methods of estimating potential evaporation	49
Figure 18. FAO 56 Evapotranspiration and EWM pan measurement	52
Figure 19. Correlation between EWM pan measurement and Penman equation.....	54
Figure 20. Correlation between simplified Penman equation and Penman equation.....	54
Table 1. Details of EWM pan and UFA raingauge measurements	38

1. Introduction

Evaporation is an important element of hydrological cycle. Its accurate estimation has been utilized quite frequently in irrigation and hydrological engineering. The history of studying evaporation phenomenon dates back to the 19th century (Chen et al 2005). Since then, many methods have been developed to achieve better understanding and better estimation of evaporation. Most of them require input of one or more weather variables or other measurements.

Putting aside the sophisticated eddy-correlation or aerodynamic methods (Monteith and Unsworth, 1990), it is mainly the pan measurement that has been attracting the attention of professional public over almost a century (Chow, 1964). It has been considered a reliable and commonly applicable method, because the evaporation rate from a pan responds to climatic factors similar to those affecting the natural water bodies and it can be obtained easily. However, the pan measurement might be affected by the artificial pan material, its small size and different exposure to the environment, so that its heat storage and convection and its radiation and aerodynamic characteristics differ from those of the natural water bodies, especially the large ones. Because of these effects, it is necessary to apply a correcting factor that is dependent on climate, geographical latitude, season, actual weather (in particular wind speed and air humidity), environment, fetch etc.

Another group of methods requires a computation, based on empirical or semi-empirical relations between the water evaporation or potential evapotranspiration rates on the one hand and various weather elements on the other hand. Belonged to this group, the theory developed by Penman (1948) which involved several meteorological factors was the most widely recommended and used worldwide. Adapted from the Penman classical theory, Penman and Monteith developed the FAO 56 combination equation (Allen et al., 1989), which has been recognized as a worldwide standard for estimation of reference evapotranspiration, but difficulties appear at many sites because of insufficient or complicated data. As a result, depending on the available data acquired at particular sites, other empirical models are used as substitutes to the combination equation, or some of the combination equation inputs have to be derived indirectly. However, as there are intricate interactions among variables and factors involved in evaporation process, most of the empirical and semi-empirical models, unavoidably relying on explicit or implicit simplifying assumptions, are less accurate, especially when they are not locally calibrated and when one tries to use them for short periods of time. Some methods can be only be used in the climatic condition similar to those

prevailing in the area of original research, while some other only provide a rough approximation irrespective of the location. The application of any empirical equation to a new location requires adjustments.

In this study the net water surface evaporation was derived from the EWM evaporation pan continuous measurement and, the performance of the pan measurement was evaluated by comparing it with the Penman equation and necessary adjustments of the latter were proposed. The EWM pan data was used to check the compatibility of one derived equation from Penman's theory in the study area. Also from the meteorological data available, the reference evapotranspiration was estimated according to the FAO 56 Penman – Monteith equation and a pan coefficient was derived.

2. Scientific hypotheses and objectives of work

The following hypotheses lies in the background of this project:

- (1) The classical Penman equation for water surface evaporation can be closely related to the EWM pan evaporation measurements; any adjustments of the former, if necessary, are easy to apply and do not vary much with location, season and other factors.
- (2) The net EWM pan evaporation can be derived in a feasible way from the gross data, taking into account the precipitation measured with a standard tipping bucket raingauge.
- (3) The EWM pan evaporation data are meaningful even on the time scale shorter than one day.

The objectives of this study are:

- (1) To find out if and to what extent the EWM evaporation pan, the Penman equation and the Penman simplified give correct values of water surface evaporation.
- (2) To elaborate an optimum method for correcting the gross evaporation data for the effect of precipitation.
- (3) To explore the variation of water surface evaporation over the diurnal period and over longer time intervals.

3. Literature Overview

3.1. Definitions

Evaporation is the process converting the liquid water at the liquid-gas interface to vapor water, which is then being removed from the evaporating surface by processes such as molecular and turbulent diffusion in the gas phase. Typical evaporating surfaces in nature are oceans, seas, lakes, rivers, puddles, raindrops, soils, vegetation and man-made structures such as roofs, pavements, ditches, canals, reservoirs and irrigation facilities.

The processes of evaporation can be categorized using the following terms, based mainly but not exclusively on the division given in Guidelines for Meteorological Instruments and Methods of Observation (WMO, 7th edition, 2012).

Evaporation characterizes the vaporization of water from water or ground surface or indeed any other surface. Non-wetted surfaces of living organisms, particularly vascular plants, are exempted from this category in its narrower sense.

Transpiration is the process during which water is transferred through the vegetation to the leaves after being taken up by the root system, then evaporating into stomatal cavities and diffusing in the vapor form through stomatal pores into the outer atmosphere.

Evapotranspiration is a superposition of evaporation and transpiration from a land patch consisting of both vegetation and other evaporating surfaces (such as soil).

Potential evaporation considers the water evaporated from pure planar water surface or another completely wet surface under existing atmospheric conditions.

Actual evaporation is the amount of water evaporated from the surface that need not be completely wet (such as a partially dried soil surface). Surfaces of living organisms, particularly vascular plants, are exempted from this category in its narrower sense.

Potential transpiration is the maximum transpiration that can be observed under existing atmospheric conditions when the plant roots are sufficiently supplied with water. In the narrower sense, the transpiration is potential when the plants do not suffer from either water stress any other stress.

Actual transpiration is the amount of water actually transpired where the plants need not necessarily be sufficiently supplied with water or free from another stress.

Potential evapotranspiration represents the quantity of water evaporated from a vegetated field surface with sufficient water supply. Some interpretations require that the soil surface must be totally covered by vegetation.

Actual evapotranspiration regards the water evaporated from the soil and plants when the ground is at its actual (not necessarily optimal) moisture content and the water status of the plants is not necessarily optimal, either. According to some interpretations, the actual evapotranspiration can be over short time higher than the potential one, e.g. after rain or irrigation, when the plant surfaces are wet.

Reference crop evapotranspiration (Allen et al. 1998) is a special case of potential evapotranspiration, defined as the amount of water evaporated from a hypothetical grass reference crop with an assumed crop height of 0.12 m, a fixed surface resistance of 70 s m^{-1} and an albedo of 0.23. This closely resembles an extensive surface of green, well-watered grass of uniform height, actively growing and completely shading the ground. The soil surface is moderately dry, resulting from about a weekly irrigation frequency.

Owing to this classification, the evaporation process is specified with respect to the type and properties of the evaporating surface and to the water resources available.

3.2. Units and scales:

The processes defined in the previous section are usually interpreted in terms of rate of evaporation (or transpiration or evapotranspiration), which is the amount of water evaporated from a unit surface area per unit time. Its dimension is mass or volume of liquid water per area, usually the depth of liquid water, per unit time, very often per day. Typical units are millimeters per day and the acceptable accuracy is 0.1 to 0.01 mm d^{-1} .

The rate of evaporation depends on two groups of factors, namely the meteorological factors and the surface factors. The former group consists of the energy supply rate and the aerodynamic variables, as water needs energy (from solar and terrestrial radiation and from the heat storage of soil, water and atmosphere) to evaporate, while aerodynamic processes (such as diffusion, turbulence and buoyancy) and the vapor pressure gradient are needed in order to remove water vapor from the surface.

The latter group of factors considers the presence or absence of free water surface as well as other surface characteristics, such as albedo, surface roughness, size and shape of the surface, soil surface wetness and the type and parameters of vegetation (height, density, coverage, leaf area index, stomatal conductance etc). The transpiration from a vegetation canopy is deeply affected by the degree of openness of stomata (which release more water vapor when they are more open and vice versa). The stomata open and close in response to

the availability of soil moisture, atmospheric conditions (especially temperature and humidity) and the diurnal cycle (WMO, 7th edition, 2012).

It must be remarked that thinking of the process of evaporation in nature along the line factors-consequences is not fully adequate, because there exists a strong feedback from the consequences towards the factors. The evaporating surface makes the warm and dry air moister and cooler and is itself becoming warmer and drier. The intensity of the feedback depends on the scale of consideration. Large homogeneous areas may be brought to a relatively perfect dynamic equilibrium with the overlying atmosphere. This fact gave rise to the so-called “complementary” or “advection-aridity” evaporation theories. Bouchet(1963) proposed the hypothesis of strong interrelationship between potential and actual evapotranspiration in a large and homogeneous territory with minimal advection of heat and moisture. In the paper by Ramirez et al. (2005), a direct observations was presented as strong evidence for this complementary relationship that was based on 192 data pairs (ET_{pan} and the water-budget based ET_a^*) from 25 basins in the USA. While ET_{pan} resulted from direct measurements, ET_a^* was the difference between precipitation and runoff. Both ET_{pan} and ET_a^* approached ET_{wet} (wet environment evapotranspiration) in the wettest basins, which strongly agrees with the Bouchet’s hypothesis. From the theory of Bouchet, the advection-aridity (AA) model was developed by Brutsaert and Stricker (1979), aiming at reliable estimation of actual evapotranspiration from few available climatic parameters. A loosely similar algorithm was independently developed by Morton (1983). Most attempts in this direction related to evaporation from large homogeneous territories over relatively long intervals (such as months or years). More recently, attempts have been undertaken to use the complementary theory for short periods (Crago, 2005).

3.3. Physical principles of evaporation

Evaporation and evapotranspiration act in accordance with several physical rules, namely the conservation of mass, momentum and energy, the gas state laws (applied to air and water vapor), the latent heat law of phase change and the transport laws (including, in particular, the molecular and turbulent diffusion).

It is universally known that, in a closed system, mass and energy can be neither created nor destroyed, but can change the location or change into other forms. When it comes to the evaporation of water, the amount of water evaporated can be determined by the mass balance of the water cycle. In term of energy, evaporation process requires energy to overcome the

intermolecular interactions (i.e. the van der Waals force and hydrogen bonds) which for water are much higher than for many other substances. This energy is called the latent heat of evaporation, since the process when liquid water absorbs energy and transforms itself into gaseous phase is endothermic process and can take place without a change in temperature. In meteorology, the part of surface energy balance that causes water to evaporate is the leaving the evaporating surface as the latent heat flux and is an important component of the energy balance equation:

$$R_n = G + H + \lambda\rho E \quad (1)$$

where R_n is the net radiation, G is the soil (or water) heat flux, H is the sensible heat flux and λE is the latent heat flux with λ being the latent heat of evaporation (which approximately equals 2.45MJ kg^{-1} when the temperature is not much different from 20°C), ρ is the density of water (kg l^{-1}) and E is the evaporation rate (mm d^{-1}). The units of the other terms in (1) are $\text{MJ m}^{-2} \text{d}^{-1}$.

The movement of water vapor flow in the open air is almost always turbulent, which means that air eddies containing different amounts of water vapor and also having different temperature and momentum spontaneously create due to inertia and move in a random way. This process is similar to the movement of molecules during molecular diffusion. It is therefore called “turbulent diffusion” and it is acceptable to apply the equations similar to those for molecular diffusion to the transport of water vapor in the atmosphere (Dolezal, 1994).

In brief, the condition *sine qua non* for evaporation process are a supply of energy to provide the latent heat of vaporization, vapor pressure gradient and turbulent (or molecular) diffusion for removing the vapor once produced (Lecture on Evapotranspiration). Dated back to 19th century, the English scientist John Dalton formulated this statement in his equation which, in today’s notation and using the basic SI units, is:

$$PE = f(u, z)(e_s(T_{ws}) - e_a) \quad (2)$$

where PE is the potential evaporation from free water surface (m s^{-1}), $e_s(T_{ws})$ is the saturated vapor pressure at the water surface temperature (Pa), e_a is the vapor pressure at a certain height above the water surface (Pa), $f(u, z)$ is the turbulent exchange function that depends on the mixing characteristics of the air above the evaporating surface ($\text{m s}^{-1}\text{Pa}^{-1}$), and u is the wind speed (m s^{-1}) at the height z (m).

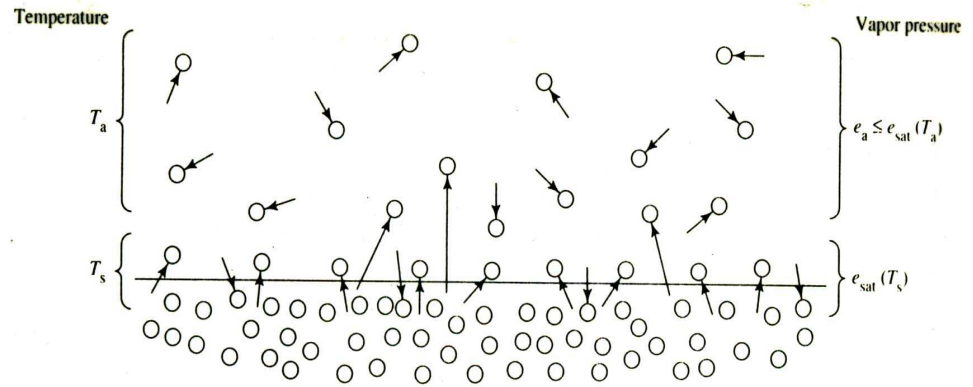


FIGURE D-4
Schematic diagram of flux of water molecules over a water surface. The vapor pressure at the surface is $e_{\text{sat}}(T_s)$; the vapor pressure of the overlying air is less than or equal to $e_{\text{sat}}(T_a)$. The rate of evaporation is proportional to $[e_{\text{sat}}(T_s) - e_a]$ [Equation (D-10)].

Figure 1. Movement of water molecules over a water surface

(<http://search.boisestate.edu/?q=evapotranspiration&site=boisestate.edu>)

Once the turbulent function is determined, it is not difficult to solve the Dalton equation. Dalton's theory can be applied to quantify the actual evaporation from bare soil or evapotranspiration from plant canopy based on exactly the same principle. Once the soil surface vapor pressure is known and the turbulent exchange function is assumed to be the same as that over water surface, we have (Wilson et al., 1997):

$$AE = f(u, z)(e' - e_a) \quad (3)$$

with AE being the actual evaporation ($\text{m}\cdot\text{s}^{-1}$), e' the actual vapor pressure at the soil surface (Pa) and e_a the vapor pressure in air. When the soil surface is smooth, the turbulent exchange function $f(u, z)$ can be considered to behave like in case of a water evaporation pan, while e' requires more effort to compute than $e_s(T_{\text{ws}})$ (Mekonnen et al, 2012). However, the wind function for evapotranspiration is much more complex, as the effect of surface roughness on turbulent boundary layer must be accounted for.

3.4. Measurements

According to Allen et al. (1998), evaporation or evapotranspiration can be measured at a small scale to represent a larger area or computed from available meteorological data. Based on the physical principles behind the process, various ways of measurement and computation were developed for different situations.

(a) Energy balance and micrometeorological methods

Energy is the factor governing evaporation and evapotranspiration. So, the processes must follow the law of energy conservation. There are methods of evaporation estimation based purely on the energy balance. In these methods, however, it is very difficult to independently estimate the sensible heat flux component. On the other hand, there are also pure mass transfer methods, which consider the vertical movement of air parcels driven by the gradients of wind speed and water vapor concentration or partial pressure, without resorting to energy balance considerations. It is, however, more advantageous to combine the two approaches, which gives rise to so-called combination methods. In addition, there exists a method that directly measures the water vapor flux in the atmosphere (the eddy correlation method) without resorting to either energy balance or the aerodynamic profiles. All these methods are most applicable in research and their direct use in practice is difficult, because of complicated data requirements.

(b) Water balance

The water balance method regards evapotranspiration as one of the components of water balance of the site. The procedure can be simplified by neglecting insignificant factors. For the soil profile case, the evapotranspiration ET can be estimated as:

$$ET = I + P - \Delta RO - DP + CR - \Delta SF - \Delta SW \quad (4)$$

with the balance inputs I (irrigation), P (precipitation), CR (capillary rise from below) and the outputs, in addition to the evapotranspiration itself, including the surface runoff ΔRO , deep percolation DP , horizontal subsurface runoff ΔSF and the increase in the soil water content ΔSW over the balance period. The surface runoff ΔRO and the subsurface runoff ΔSF are actually differences between runoff and run on (mathematically speaking, divergences of the respective vector fields). This method typically expects observations over weekly or ten-day periods over which all balance terms can be estimated with a reasonable accuracy. A similar water balance approach can be applied on the scale of a drainage basin or a lake.

(c) Evaporation pans

Basically, the evaporation pans or tanks simulate all processes involved in evaporation from natural water bodies. According to Guidelines for Meteorological Instruments and Methods for Observation (WMO, 7th edition, 2012), pans can be made in different shapes and

sizes, from the Russian 20m² tank to the smaller Russian GGI-3000 pan with the cross-section of 3000 cm² and the US Class A pan with the diameter of 120.7 cm and the cross section 11 442 cm², respectively. The pans or tanks can be operated in three different positions in relation to the surrounding surface:

- Sunken pans or tanks which have most of the equipments below the ground surface;
- Above- ground pans or tanks are those placed at small height above the ground;
- Pans mounted on floating platforms.

In general, the pan evaporation measurement is the simplest way to quantify the water gain and loss due to weather conditions. It is easily operated and easily available in any place and time (except for the periods of frost). However, there are some typical errors experienced with them, associated with their size, placement and other operational characteristics. The above-ground pans often overestimate the amount of water evaporated as the result of the additional energy absorbed by their sides, the sunken pans or tanks may provide unreliable data because of untraceable leakage and the floating pans can gain or lose water due to wind and waves. Besides, all types of pans are also subject to the errors caused by extreme weather events, birds and animals.

(d) Lysimeters

Lysimeter is a water-balance based instrument used for measuring evapotranspiration, as well as for investigating percolation and leaching of various substances from the soil. The instrument physically simulates the soil water mass balance for a finite amount of soil, usually with the lateral flows excluded. It considers the water gain from rain events or irrigation and the loss by percolation and evapotranspiration, while the change in water storage is also considered.

(e) Computing evaporation from meteorological data

A broad and heterogeneous group of evaporation estimation methods is based on empirical or semi-empirical equations involving weather data, while avoiding field measurements of liquid water or soil water. Several such methods are named after their inventors, e.g. Thornthwaite (1948), Hamon (1961), Thornthwaite, Blaney-Criddle (Doorenbos and Pruitt, 1977) or Hargreaves (see below). Majority of input data for these methods are temperatures which are the most basic data for any meteorological stations.

Xu et al. (2001) evaluated and compared the most widely used temperature based methods for evaporation estimation. The simplest Thornthwaite equation correlates average monthly temperatures with evapotranspiration. The correlation was first studied in the east central USA, where valleys had sufficient moisture. The standard potential evapotranspiration ET' (mm) was derived as:

$$ET' = C \left(\frac{10T_a}{I} \right)^a \quad (5)$$

where I is the annual heat index, being a sum of monthly heat indices i_j :

$$i = \left(\frac{T_a}{5} \right)^{1.51} \quad (6)$$

and $C = 16$, $a = 67.5 * 10^{-8} I^3 - 77.1 * 10^{-6} I^2 + 0.0179 I + 0.492$ and T_a is average monthly temperature ($^{\circ}\text{C}$)

From then, the potential evapotranspiration in a particular month ET (mm) was determined with the additional information of number of days N in month and the average monthly daylight hours d :

$$ET = ET' \left(\frac{d}{12} \right) \left(\frac{N}{30} \right) \quad (7)$$

Another approach mentioned by Xu et al.(2001) is the Blaney-Criddle method, with the ET (mm) estimated as:

$$ET = k_p(0.46T_a + 8.13) \quad (8)$$

In equation (8), T_a is mean temperature ($^{\circ}\text{C}$), p is average relative daylight hours for the period used (daily or monthly) out of total daylight hours of a year (365×12) and k_p is the monthly consumptive use coefficient that is dependent on the vegetation cover, location and season, ranging from 0.5 to 1.2.

Besides, Hargreaves and Hamon methods also use similar temperature-based approaches. Among the several equations proposed by Hargreaves, Xu et al. (2001) discuss the version by Hargreaves and Samani (1982;1985):

$$ET = 0.0023 R_a T D^{1/2} (T_a + 17.8) \quad (9)$$

where R_a is extraterrestrial radiation (in equivalent evaporation unit), $TD(^{\circ}\text{C})$ is temperature difference between the mean monthly maximum and minimum, T_a is the air temperature ($^{\circ}\text{C}$).

Hamon's (1961) equation is as follows:

$$ET = 0.55D^2Pt \quad (10)$$

where ET is the average monthly potential evapotranspiration (in d^{-1}), D is the mean monthly daylight hours (in units of 12 hours) and Pt is saturated vapor density given by the formula:

$$Pt = \frac{4.95e^{(0.062T_a)}}{100} \quad (11)$$

where T_a is the air temperature ($^{\circ}\text{C}$).

Evaluation of these methods showed that a large bias could be expected if no adjustment is made for the particular study area, as a consequence of the location specific empirical constants applied in the original formulae. By using calibration with the pan measurement, all equations represent a reasonable estimation of seasonal evaporation value. Another group, so-called radiation methods, uses the solar radiation as the main input. The Makkink formula (Doorenbos and Pruitt, 1977) is a typical example.

A special place within this group is occupied by the combination methods based on the Penman (1948) approach, which in principle is exact rather than empirical and relies on a combination of the aerodynamic and the energy balance methods, made easier due to local linearization of the saturated vapor pressure curve.

Regarding the sensible heat flux H , Penman suggested to use the same turbulent exchange function:

$$H = \lambda \gamma f(u, z)(T_{ws} - T) \quad (12)$$

where γ is the psychrometric constant ($\text{kPa } ^{\circ}\text{C}^{-1}$); λ is the latent heat of vaporization (MJ kg^{-1}), $f(u, z)$ is the turbulent exchange function ($\text{mm d}^{-1} \text{kPa}^{-1}$).

Substituting (13) into the energy balance equation (1) together with the Dalton equation (1) will form the well-known Penman equation for potential evaporation from water surface, in our notation:

$$E = \frac{\frac{\Delta(T)(R_n - G)}{\lambda\rho} + \gamma f(u, z)(e_s(T) - e)}{\gamma + \Delta(T)} \quad (13)$$

where E is the potential evaporation (mm d^{-1}), R_n is the net radiation ($\text{MJ m}^{-2} \text{d}^{-1}$); G is the soil heat flux which is often neglected for daily interval; Δ is slope of the saturation vapor pressure curve ($\text{kPa } ^\circ\text{C}^{-1}$), γ is the psychrometric constant ($\text{kPa } ^\circ\text{C}^{-1}$); λ is the latent heat of vaporization (MJ kg^{-1}), ρ is the density of water (kg/liter), D is water vapor pressure deficit (kPa), $f(u, z)$ is the turbulent exchange function ($\text{mm d}^{-1} \text{kPa}^{-1}$), in this case the Penman's empirical wind function $f(u, z) = a_u + b_u u_2$, with a_u and b_u are constant coefficient and u_2 the wind speed at 2 m. The units of u_2 determine the values of a_u and b_u .

The theory of Penman opened the possibility to modify the water evaporation equation so that it also describes the evapotranspiration from a vegetation canopy or evaporation from bare soil. Since 1948, several researchers have been successful in creating similar formulae, some of which have been applied widely, especially in the field of irrigation management.

Monteith (1965), relying on Penman's ideas, solved the problem for the vegetation canopy. In that case, the latent heat flux is smaller than from the water surface, because of the additional stomatal resistance. Mekonnen et al. (2012) reformulated the Penman-Monteith equation, taking the turbulent exchange function for latent the heat flux, named $g(u, z)$, different from that for the sensible heat flux, $f(u, z)$. Then a derivation similar to Penman's or Penman-Monteith's led to the reformulated Penman-Monteith equation for actual evapotranspiration AE :

$$AE = \frac{\frac{\Delta(T)(R_n - G)}{L\rho} + \gamma f(u, z)(e_s(T) - e)}{\frac{\gamma f(u, z)}{g(u, z)} + \Delta(T)} \quad (14)$$

where the other symbols and their units are the same as in the Penman equation (14). Usually, however, the Penman-Monteith equation is written in terms of resistances (namely, the aerodynamic resistance r_a and the surface resistance r_s) instead of the exchange functions $f(u, z)$ and $g(u, z)$.

There also exists a theory applying the Penman's approach to evaporation from a partially dried soil surface, the so-called Penman-Wilson equation (Wilson et al., 1997). Omitting the aerodynamic part of the Penman equation leads to the Priestley and Taylor (1972) equation, approved to be suitable for large well-watered areas. Allen et al. (1998)

adopted the Penman-Monteith equation with a fixed value of canopy resistance as a standard method for evaluating crop water requirements. Since then, this so-called FAO 56 combination equation became one of the most widely used methods for the potential evapotranspiration estimation. This so-called “reference crop evapotranspiration” can be related to the actual crop evapotranspiration through the basal crop coefficient and the water stress coefficient (the former relating to standard water supply conditions and the latter to non-standard, water-stress conditions). The FAO 56 combination equation reads:

$$ET_0 = \frac{0.408\Delta(T)(R_n - G) + \gamma \frac{900}{T + 273} u_2 (e_s - e_a)}{\Delta(T) + \gamma f(u, z)} \quad (15)$$

where $f(u, z) = 1 + 0.34 u_2$ and the other symbols and units are the same as in (13) and (14).

As the FAO 56 combination equation still requires complicated meteorological data, other methods of the reference crop evapotranspiration estimation may be more advantageous if the data are insufficient (Doorenbos and Pruitt, 1977). Then the FAO 56 combination method can be used as a reference to obtain coefficients for correcting the results of the other methods.

3.5. Overview of previous researches

In China, several methods were used to compare with the reference FAO 56 combination method. Chen et al (2005) compared the reference method with two others: the Thornthwaite method (considering only two factors: temperature and day of the year) and the pan measurement. As predicted, the Thornthwaite method showed large bias because it neglects other variables like wind speed, solar radiation or humidity, which also play important role in ET determination. In particular, the results from the Thornthwaite method overestimated ET_0 when the evapotranspiration was low and vice versa. Moreover, it did not follow the actual temporal variation of evapotranspiration. At the same time, ET_0 reported by various types of pan measurement expressed considerably similar temporal variation to the calculation of FAO56 modified Penman-Monteith equation. The matter was that the pans also consistently gave higher values than FAO 56, so as to effectively use the pan data, correction factors (pan factors K_p) must be introduced. This was done by Chen et al. (2005) for major rivers in China. These correction factors were ranging from 0.4 to 0.8. Briefly, this research proved that the pan measurement could be an alternative solution to the complex FAO56 formula. According to Jensen (2010), similar pan coefficient ranges have been accepted

worldwide, and even when there are no data for a more accurate approximation of K_p , the value of 0.7 is acceptable.

Besides various efforts to determine and adjust the pan evaporation E_{pan} for obtaining the reference crop evapotranspiration, emphasis has been recently put on the short term energy and water balance of the evaporation tank. Martinez et al. (2004) made simulations of evaporation from a pan based on the value of the surface temperature and an empirical mass transfer equation. This research regarded two possibilities: an evaporation pan with multi-layered water temperature and a pan with thermal stratification negligible. The outcome of the research proved that there is no evidence of thermal stratification within the water: during the day, water in pan is mixed well as a result of wind speed, while at night low wind and natural convection due to radioactive cooling homogenize the water temperature. Hence, it is practical to simulate evaporation from a pan with the assumption of homogenous water temperature. However, the multi-layered model could be effectively be used for extrapolation of evaporation from deep and large water bodies.

Although the FAO 56 formula had been recognized for its accuracy for estimation of ET_0 , the large number of meteorological data required as input might not be always available, especially in conventional agrometeorological stations. To cope with that, there have been various research efforts attempting to correlate ET_0 to other, easily obtained data. One often encountered solution was to simplify the FAO 56 Penman-Monteith or the original Penman formula to the forms that require less number of meteorological data.

Valiantzas (2006) proposed an equation derived from Penman's to quantify the amount of water evaporation E_{pen} based on normal weather data at the elevation $z = 0$ a m.s.l. This equation is referred to below as "simplified Penman":

$$E_{pen} \approx 0.051(1-\alpha)R_s\sqrt{T+9.5}-0.188(T+13)\left(\frac{R_s}{R_a}-0.194\right) \\ (1-0.00014(0.7T_{max}+0.3T_{min}+46))^2\sqrt{\frac{RH}{100}}+0.049(T_{max}+16.3)\left(1-\frac{RH}{100}\right)(a_u+b_uu) \quad (16)$$

where E_{pen} is potential evaporation (mm d^{-1}), α is the albedo, which theoretically equals 0.08 for water surface and 0.23 for the reference grass, a_u and b_u are wind function coefficients, R_s is shortwave downward radiation ($\text{MJ m}^{-2} \text{d}^{-1}$), R_a is extraterrestrial radiation ($\text{MJ m}^{-2} \text{d}^{-1}$), T_{max} , T_{min} is maximum and minimum temperature, respectively ($^{\circ}\text{C}$), RH is relative humidity (%) and u is wind speed at 2m height (m s^{-1}).

Valiantzas (2006) also brought out another option for the case when the data on wind speed are not available at all or are of questionable integrity:

$$E_{pen} \approx 0.047R_s\sqrt{T+9.5} - 2.4\left(\frac{R_s}{R_a}\right)^2 + 0.09(T+20)\left(1 - \frac{RH}{100}\right) \quad (17)$$

Where T is mean temperature ($^{\circ}\text{C}$)

The later equation showed good resemblance to the former one. The relative error of these equation was 4% when compared to the standard Penman equation for water surface evaporation. A similar comparison was conducted to observe the effect of real elevation. Linear regression indicates a simple relationship between the $E_{pen} = E_{z=0}$ value at $z=0$ and the corresponding E_{pen} value at a real elevation z , which can be expressed as:

$$E_{pen} \approx E_{z=0} + 0.00012z \quad (18)$$

where z is the elevation of the area of interest (m).

Similarly, the FAO Penman-Monteith formula for the reference crop evapotranspiration was simplified by Valiantzas (2006), with the following result for the wind speed data included:

$$ET_0 \approx 0.051(1-\alpha)R_s\sqrt{T+9.5} - 2.4\left(\frac{R_s}{R_a}\right)^2 + 0.048(T+20)\left(1 - \frac{RH}{100}\right)(a_v + b_v u) + 0.00012z \quad (19)$$

Besides the articles related directly to the topic of this thesis, several other papers are reviewed below to provide more insight into the current trends in evaporation research. M.Cobaner (2011) used the wavelet regression technique. The wavelet transform is a method of analyzing non-stationary signals of data simultaneously in the frequency and the temporal/spatial domains. It, however, has become an effective tool for analyzing the variability of hydrological processes and the impacts of climatic variation on these processes. The wavelet transform has proved to be able to reveal correlation (or coherence) between evapotranspiration estimates and weather data. In his study, Cobaner (2011) analyzed three empirical models used for estimating ET_0 and the Class A pan measurements.

To deal with the lack of data in local evaporation studies, Keskin (2004) introduced the fuzzy logic theory. Although first utilized for processing uncertainties in decision making, its application areas later broadened to the field of estimation, prediction, control, optimization, etc. The principle of the fuzzy logic is that any statement is only partially true/wrong. In

evaporation modeling, the factors relating to this process, including temperature of air and water, solar radiation, air pressure, sunshine hours, wind speed and relative humidity, were ordered according to their correlation coefficients to the pan evaporation. From the basic physical relationships among these factors, it was easy to define extreme conditions. Then the intermediate functions were formed based on the existing data from 2001 and the logical ruling function. To examine the accuracy of the model, Keskin compared the results of the model and the Penman method to the pan measurement data. The outcome of this research was that the fuzzy model provided values more closely related to the pan measurement than the Penman method. Hence, fuzzy models could effectively help predict evaporation rates in the high and low evaporation periods.

4. Materials and methods

4.1. Study area

The study area is the experimental site of the Department of Water Resources, Faculty of Agrobiological Sciences, Food and Natural Resources, Czech University of Life Sciences, Prague 6-Suchbátar, north-west of Prague. The site lies at 14°22'E and 50°08'N and at 281 m a.s.l.

Long-term weather data can be taken from several weather stations in the surroundings, such as, for example, Prague-Ruzyně or Prague-Karlov. The monthly weather data for these stations are available from the Czech Hydrometeorological Institute since 1961. Long term averages are suitable to characterize the climate, because they smooth over the short-term fluctuations. Over the period 1961-2000, the mean annual precipitation and temperature as observed in Prague-Karlov were 431 mm and 9.3°C, respectively (Historical weather data in Prague).

4.2. Models

In this study, the water surface evaporation was estimated based principally on the processing of pan measurement data. In addition, the daily pan evaporation sums were compared to four models mentioned in the literature review, namely:

- The Dalton's equation
- The Penman equation for potential evaporation
- The Penman simplified equation for evaporation rate
- FAO 56 Penman-Monteith equation for reference crop evaporation

The parameters of these models were then optimized to fit the best with the measurement data and compared with their original values.

4.3. Measurements

4.3.1. Measurement of potential evaporation

The potential (water surface) evaporation was measured at the experimental site by an EWM pan, the geometry of which is derived from the standard Russian evaporation pan GGI-3000. It belongs to the sunken-pan group. The pan is of cylindrical design, made of stainless steel, with 3000 cm² cross-sectional area and 60 cm height.



Figure 2. EWM pan



Figure 3. Optical sensor of EWM pan

The EWM pan was developed by AS & Consulting, Mělník, Czech Republic and is in standard use by the Czech Hydrometeorological Institute (Mekonnen et al., 2012).

Attached to the pan is an automatic water-level measuring device, placed in a 7.5 cm radius stainless steel vessel with a lid. Water level in the vessel is detected by a float and monitored by a digital optical position sensor with 0.1mm resolution. Due to evaporation or precipitation, the float falls or rises respectively. After every 24 hour, the EWM pan is restarted automatically and water is pumped in or out to re-establish a zero standard level.

Surface water temperature in the pan was measured by a Pt100 resistance sensor, kept immediately under the water surface by a special float.

Data on both water level and water surface temperature at 10-minute intervals were transformed into a digital form by a collecting unit and then recorded by a DT80 (data Taker Pty.) data logger.

The EWM pan evaporation measurements processed in this thesis comprise two and a half growing seasons, namely, the periods (with some gaps):

- Year 2010: From 7/30/2010 to 11/23/2010.
- Year 2011: From 4/23/2011 to 11/12/2011
- Year 2012: From 4/25/2012 to 10/26/2012

Main outcomes for training sample (May 2011) and for the year 2010 (or 2011) are presented below in the Results section of the main text, while the other results were put in the Appendix.

4.3.2. Measurement of precipitation



Figure 4. Tipping bucket raingauge

An automatic tipping bucket rain gauge (type MR3H from Meteoservis, v.o.s, Vodnany, Czech Republic, operated by the Institute of Atmospheric Physics, Academy of Sciences) was employed to measure precipitation in the experimental field at the height 1 m above the ground. The rain gauge was placed at about 10 m distance from the evaporation pan. It consists of two compartments balanced in unstable equilibrium; rain water accumulated in one compartment causes the bucket to tilt over after being filled with a defined amount of water. The tips produced in this way are recorded. Each tip corresponds to 0.1 mm of precipitation. Precipitation sums over 10-minute intervals are then automatically calculated by interpolation. Besides the tipping bucket rain gauge, the data from small-size manual rain gauges for daily total precipitation measurement at the ground level were used for comparison.

4.3.3. Measurements of atmospheric variables

To make a comparison of pan data with the theoretical models possible, other data measured on the site were also used, namely the solar radiation, the air temperatures (dry and wet-bulb), wind speed and relative humidity of air.

The air temperatures were measured by Pt100 resistance sensors placed at 2 m height in a small weather screen. One of these sensors, serving as the wet-bulb thermometer, was wrapped with a textile sleeve immersed in a bottle with distilled water, which used to be re-filled regularly. The temperatures were transformed into a digital form by a collecting unit and then recorded by a DT80 data logger. In parallel, a temperature and humidity sensor combined probe HMP 45A/D by Vaisala, Helsinki, Finland was placed at 2 m height in another weather screen at few meters distance. Its data were recorded by an independent data logger. The latter equipment was supplied by Meteoservisand operated by the Institute of Atmospheric Physics, Czech Academy of Sciences.



Figure 5. Pyranometer

The downward short-wave radiation was measured directly by the pyranometer (LP02 Hukseflux) at a reference height 2m above the ground surface. The data were recorded at 10-minute intervals by the DT80 data logger.

The wind speed was measured by a MetOne 034B anemometer at 10 m above the ground and a more reliable ultrasound wind speed and direction sensor Windsonic from Gill Instruments Ltd., Hampshire, UK, placed at 2 m above the ground, the latter operated by the Institute of Atmospheric Physics, Czech Academy of Sciences. The data of both anemometers, placed at few meters distance from each other, were recorded at 10-minute intervals.

However, all Institute of Atmospheric Physics data (tipping bucket precipitation, air temperature and relative humidity, ultrasound wind speed) were recorded at 15-minute

intervals over the first half of 2010 and had to be later converted into 10-minute intervals by linear interpolation.

4.4. Basic data processing

4.4.1. Temperature

The average daily dry-bulb and wet-bulb temperatures were calculated as:

$$T_{dry} = \frac{\sum_{i=1}^n T_{dry,i}}{n} \quad (20)$$

$$T_{wet} = \frac{\sum_{i=1}^n T_{wet,i}}{n} \quad (21)$$

where i is the serial number of observation and n is the total number of observations qualified for calculation ($n=144$). The averages, as well as the maxima and minima, were taken over diurnal periods from 7:30 am of the actual day to 7:30 am of the following day, using the Central European (winter) time.

4.4.2. Vapor pressure

Vapor pressure is the partial pressure caused by water vapor molecules in the atmosphere. Saturated vapor pressure e_s is related to temperature T through the formula (Allen et al., 1998):

$$e_s = 0.6018 \exp\left[\frac{17.27T}{T + 237.3}\right] \quad (22)$$

where T is the temperature ($^{\circ}\text{C}$) and e_s (kPa) is the saturated vapor pressure corresponding to the temperature T .

Similarly, the average daily saturated vapor pressures were taken as the averages of 10-minute data series as:

$$e_s = \frac{\sum_{i=1}^n e_{s,i}}{n} \quad (23)$$

The average daily values of the water surface temperature T_{ws} in the EWM pan and the corresponding average daily saturated vapor pressures $e_s(T_{ws})$ were estimated in the same way:

$$T_{ws} = \frac{\sum_{i=1}^n T_{ws,i}}{n} \quad (24)$$

$$e_s(T_{ws}) = \frac{\sum_{i=1}^n e_{s,(T_{ws}),i}}{n} \quad (25)$$

The actual vapor pressure can be obtained either from the relative humidity data or from the psychrometric (wet and dry bulb) data. If the relative humidity data are used, then the average daily water vapor pressure e_a is calculated according to FAO 56 recommendation (Allen et al., 1998) as:

$$e_a = \frac{e_s(T_{\min}) \frac{RH_{\max}}{100} + e_s(T_{\max}) \frac{RH_{\min}}{100}}{2} \quad (26)$$

where RH_{\max} and RH_{\min} are the maximum and minimum relative humidity (%) over the corresponding diurnal period.

When the psychrometric data are used, then the average daily air pressure is obtained from the average daily dry-bulb and wet-bulb temperatures Allen et al., 1998):

$$e_a = e_{s,wet} - \gamma_{psy} (T_{dry} - T_{wet}) \quad (27)$$

with γ_{psy} being the psychrometric constant (kPa K^{-1}), estimated as:

$$\gamma_{psy} = a_{psy} P \quad (28)$$

where $a_{psy} = 0.0008$ is the naturally ventilated psychrometer coefficient and P (kPa) is the average barometric pressure, dependent on the site elevation:

$$P = 101.3 \left(\frac{293 - 0.0065z}{293} \right)^{5.26} \quad (29)$$

with z being the site's altitude (m).

The slope of saturation vapor pressure curve was estimated as (Allen et al., 1998):

$$\Delta = \frac{4098[0.6108 \exp(\frac{17.27T}{T+237.3})]}{(T+237.3)^2} \quad (30)$$

4.3.3. Solar radiation

Besides the short-wave radiation, all other solar radiation components were derived from empirical equations recommended in the FAO 56 guidelines (Allen et al. 1998).

As the incoming solar radiation can be either absorbed or reflected, the *net shortwave radiation* (the absorbed short-wave radiation) R_{ns} was determined as:

$$R_{ns} = (1 - \alpha)R_s \quad (31)$$

where α is the albedo, which varies according to the type of surface. For calculating the reference crop evapotranspiration ET_0 , α is assigned the value of 0.23 (-).

The average daily *extraterrestrial radiation* (R_a) represents the local radiation intensity on a horizontal surface at the top of the earth's atmosphere ($\text{MJ m}^{-2} \text{d}^{-1}$). R_a is inferred from the squared inverse relative Sun-Earth distance d_r (-), the geographic latitude φ (radian), the solar hour angle at sunset ω_s (radian) and the solar declination δ (radian):

$$R_a = \frac{1440}{\pi} G_{sc} d_r [\omega_s \sin(\varphi) \sin(\delta) + \cos(\omega) \cos(\delta) \sin(\omega_s)] \quad (32)$$

$$d_r = 1 + 0.033 \cos(\frac{2\pi}{365} DOY) \quad (33)$$

$$\delta = 0.409 \sin(\frac{2\pi}{365} DOY - 1.39) \quad (34)$$

$$\omega_s = \arccos[-\tan(\varphi) \tan(\delta)] \quad (35)$$

where the solar constant $G_{sc} = 0.082 \text{ MJm}^{-2}\text{min}^{-1}$ and DOY is the Julian day.

Clear sky solar radiation at the bottom of the atmosphere R_{so} ($\text{MJ m}^{-2} \text{d}^{-1}$) is required in the absence of directly measured net radiation. It is the daily average shortwave downward radiation in the case that the actual duration of sunshine n equals the maximum possible duration of sunshine N . The equation for R_{so} (Allen et al., 1998) relates it to the extraterrestrial radiation R_a and the elevation of the weather station z (m):

$$R_{so} = (0.75 + 2 * 10^{-5} z) R_a \quad (36)$$

The average daily *net long wave radiation* R_{nl} ($\text{MJ m}^{-2} \text{d}^{-1}$), positive upwards, characterizes the balance between the long-wave radiation energy reaching the Earth's surface and the similar radiation energy leaving the surface. According to FAO 56 recommendation (Allen et al., 1989), it can be estimated from the equation:

$$R_{nl} = \sigma \left(\frac{T_{\max}^4 + T_{\min}^4}{2} \right) \left(0.34 - 0.14 \sqrt{e_a} \right) \left(1.35 \frac{R_s}{R_{so}} - 0.35 \right) \quad (37)$$

The equation (36) is applicable to the reference grass canopy, while the original equation by Penman (1948) is more suitable for water surface. The Penman equation with the original Penman's values of parameters was converted into contemporary units by Calder (1990):

$$R_{nl} = \sigma T^4 \left(0.56 - 0.248 \sqrt{e_a} \right) \left(0.9 \frac{R_s}{R_{so}} + 0.1 \right) \quad (38)$$

where T_{\max} , T_{\min} , T are the maximum, minimum and average daily absolute air temperature, respectively (K), σ is the Stefan-Boltzmann constant ($4.903 \cdot 10^{-9} \text{ MJ K}^{-4} \text{ m}^{-2} \text{ day}^{-1}$) and e_a is the actual average daily vapor pressure in the air at 2 m (kPa).

Balancing all sorts of radioactive energy at the evaporating surface gives the net radiation R_n ($\text{MJ m}^{-2} \text{day}^{-1}$), positive downwards:

$$R_n = R_{ns} - R_{nl} \quad (39)$$

4.3.4. Wind speed

Data of wind speed u , measured and recorded by an anemometer, make a key input to the estimation of the turbulent exchange function $f(u, z)$. In this thesis, I use the Penman (1948) linear wind function, which in contemporary units reads (Calder, 1990):

$$f(u, z) = 2.6(1 + 0.537u_2) \quad (40)$$

where $f(u, z)$ is the Penman wind function ($\text{mm d}^{-1} \text{ kPa}^{-1}$) and u_2 is the wind speed at 2m height.

4.4. Bridging gaps in data

During the study period, there were gaps in the records, where the data were totally missing or influenced by systematic errors. In order to make the data series continuous, these

gaps were bridged by regression to other data available. Correlation coefficients r and the determination coefficients r^2 were also calculated to express the extent to which the relation between the quantities of interest are fitted by the regression equations. The model is more accurate when both r and r^2 are high. Ideally they approach unity.

The gap bridging can be done using data from other trusted sources, as FAO's instructions for dealing with missing data recommend (Allen et al., 1998).

4.4.1. Bridging wind speed

Data on wind speed received in the experimental field were systematically very small on some particular days, which could be caused by a systematic error or the wind could indeed be very light. FAO56 suggested to take the value of 2 m s^{-1} for the days with missing values of wind speed and to raise all measured values smaller than 0.5 m s^{-1} to this value, because, on light-wind days, the water vaporization is additionally promoted by instability of the boundary layer and buoyancy of air. This procedure ameliorated the estimation of ET_0 .

4.4.2. Bridging solar radiation

FAO56 proposed several ways to recover missing data on solar radiation, of which the most suitable method is the derivation from daily air temperature differences. The reason for choosing this alternative method was that air temperature data could be considered the most reliable data series.

For strongly continental climatic conditions as those prevailing in Prague, where the air mass is not influenced heavily by the ocean, the formula (so-called Hargreaves' radiation formula) can be used (Allen et al., 1998) to estimate the solar radiation R_s :

$$R_s = 0.16\sqrt{(T_{\max} - T_{\min})}R_a \quad (41)$$

4.4.3. Bridging water temperature

While the missing dry-bulb temperature measured by the Pt100 thermometer can be easily replaced, after calibration, by the Institute of Atmospheric Physics (UFA) data, the estimation of missing data of water temperature and wet-bulb temperature involves more complex calculations.

Following the development of the Penman equation for potential evaporation from water surface, Mekonnen et al. (2012) wrote a formula for estimating the water temperature as followed:

$$T_{ws} = T + \frac{(R_n - G) / (L\rho) - f(u, z)[e_s(T) - e_a]}{[\gamma + \Delta(T)]f(u, z)} \quad (42)$$

where the meaning of the symbols is the same as in equation (13).

4.4.4. Bridging wet-bulb temperature

While estimating relative humidity from the dry and wet bulb temperature is a step-by-step process based on the psychrometric equations such as (26), the inverse task to deduce the wet bulb temperature T_w from the relative humidity and dry bulb temperature T is not easy to achieve.

Stull (2011) introduced an analytical solution for estimating the T_w by the fitting method:

$$T_w = T \arctan[0.151977(RH\% + 8.313659)^{1/2}] + \arctan(T + RH\%) - \arctan(RH\% - 1.676331) + 0.00391838(RH\%)^{3/2} \arctan(0.023101RH\%) - 4.686035 \quad (43)$$

This equation is accepted for a wide range of RH from 5% to 99 % and of air temperatures.

4.4.5 Temperature examples

At this stage, I present examples of temperature data after the primary processing which were later used as inputs for the estimating evaporation or evapotranspiration. As mentioned above, the air temperature was measured by a Pt100 resistance sensor and recorded at 10-minute intervals. Independent measurements were taken with the temperature and relative humidity sensor by the Institute of Atmospheric Physics). The latter data (referred to below as UFA) were also, for most of the time, registered at 10-minute intervals, but the interval was 15 minutes at the beginning of the period of observation. To cope with this problem, the 15-minute data were linearly interpolated in Microsoft Excel to get 10-minute interval series. All UFA data, containing information on temperature, relative humidity, wind speed and precipitation, were interpolated in this way.

The two data series on temperature were then compared and their linear regression was calculated. The DT80 data (wet bulb temperature, dry bulb temperature and water

temperature) were considered the dependent variables, while the UFA series air temperature was set as the independent variable. Although the UFA air temperature data were lower than the Pt100 air temperatures (Fig. 6), they showed high correlation between each other. Hence, the estimation of unavailable Pt100 air temperatures by regression from the UFA air temperatures can be regarded a reliable procedure.

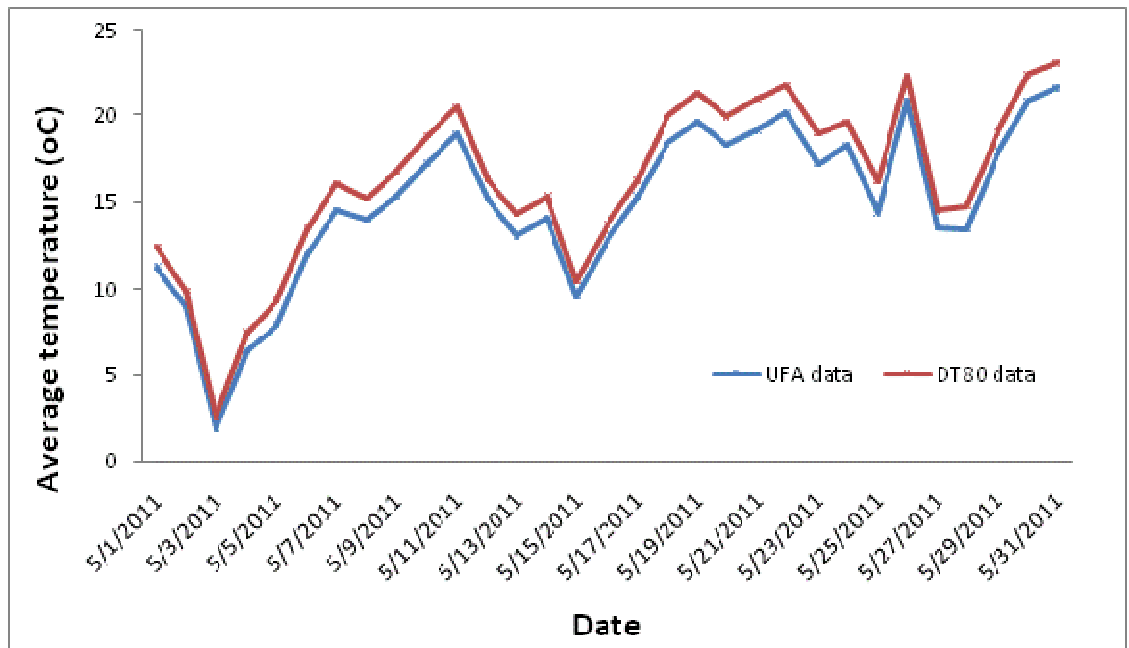


Figure 6. Pt100 (DT80) and UFA average daily air temperature comparison

Similarly, the missing Pt100 wet-bulb temperatures T_w and water surface temperatures T_{ws} were regressed to the UFA air temperatures. The water surface temperature can be estimated in this way even for the winter periods, in which the EWM evaporation pan was not operating at all. Fig. 7 depicts the temporal variation of the average daily values of air temperature (T), wet-ulp temperature (T_w) and the surface water temperature T_{ws} , directly measured by the Pt100 thermometers, with the gaps bridged by regression from the UFA air temperatures. The results are presented for the whole calendar year 2001.

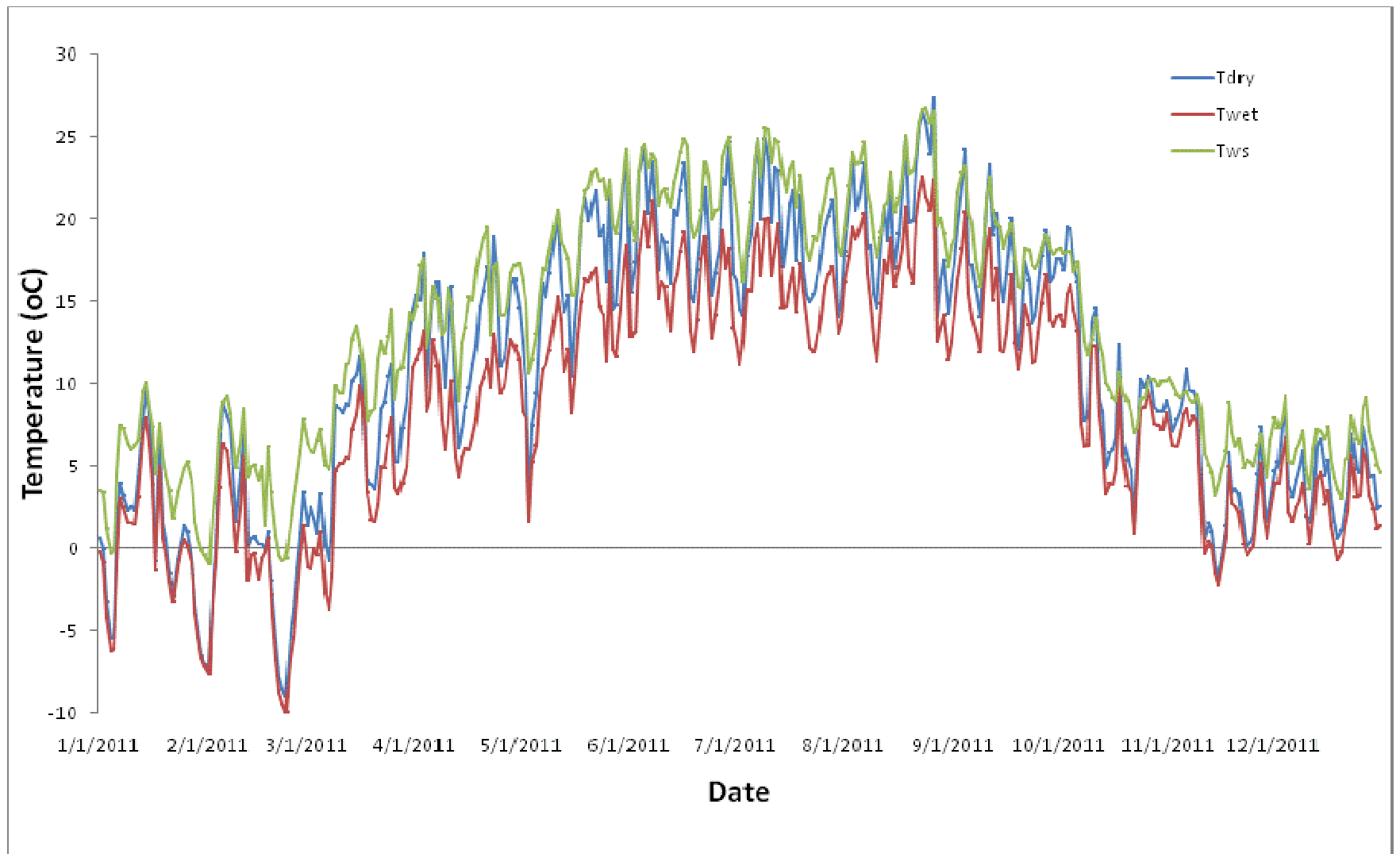


Figure 7. Dry-bulb, wet-bulb and water surface average daily Pt100 temperatures in 2011,with the gaps bridged by regression to the UFA air temperatures

As expected, on most of the days the wet-bulb temperature was the smallest, the dry-bulb temperature was in the middle and the water surface temperature was the highest. However, they kept on a consistent fluctuation path. On frost days, the data were almost exclusively obtained by regression (except for the average daily dry-bulb temperature T). On such days we observe the largest differences between the air temperature and the water temperature. Such variations could be explained by the heat storage of water in the EWM evaporation, causing the temperature of water being less variable compared to the atmospheric temperature.

5. Results

5.1. Processing pan measurements

To calculate net evaporation from EWM pan, there are two factors that need to be considered: the evaporation itself and the precipitation. According to the law of mass conservation, the amount of water evaporated from the pan can be obtained by calculating cumulative precipitation at 10-minute intervals and then subtracting it from the water level elevations in the pan (Measurement and Processing of Meteorological Data). The result is the net cumulative evaporation. It has a negative algebraic sign, because water level in the pan normally sinks down during rainless periods. The jumps in data produced by the restart of the EWM pan each morning at 7:30 CET mark natural starts and ends of both precipitation and net evaporation accumulation intervals.

Along with this seemingly obvious method (which, however, did not prove reliable for periods shorter than one day), I used another method to derive the net evaporation rate not requiring the use of precipitation data (F. Dolezal, 2012, private communication). The method relies on the fact that the pan is also able to measure the precipitation rate (if the evaporation itself is negligible), so that the effect of precipitation is already accounted for in the fluctuation of water level in pan. This procedure effectively eliminates the need of using independent precipitation measurements, except for some extreme cases. In brief, only the non-positive changes (declines) in the pan water level are accounted and added up to the cumulative net evaporation, while the positive changes (rises) are ignored.

Theoretically, the two methods (with precipitation and without precipitation) should provide the same results if the independent precipitation measurements are accurate and exactly corresponding to the precipitation that has fallen into the evaporation pan, and if the evaporation taking place during rain events can be neglected. these two conditions are not exactly fulfilled.

Examples of primary runs (in Excel) of the former method (with precipitation) for a sample period (May 2011) are presented in Appendix 1. In this and all other similar graphs in this thesis, the net cumulative evaporation is plotted with a negative sign and the cumulative precipitation with a positive sign. It soon became evident that the cumulative precipitation values were underestimated. The net cumulative evaporation, which should be a non-increasing function of time except for the instants of restart, started to increase (i.e. to become less negative) during the

rain events or even went positive when the rains were heavy, like if the water level in pan rose more during the rain than it would correspond to the amount of precipitation, which was impossible.

The problems were partially eliminated by multiplying the raingauge precipitation with a coefficient larger than unity. The optimum value of the coefficient was sought, at first by trial and error. Appendices 2 and 3 show the results when this coefficient was taken as 1.4 (too small) and 2.0 (too large), respectively. Further optimization of the coefficient showed that its value may have been simultaneously too large during some rain events and too small during others. It was then concluded that the method “with precipitation” is not suitable for estimating evaporation rates for periods shorter than one day.

The method “without precipitation” is illustrated in Fig. 8, which depicts first few days of May 2011.

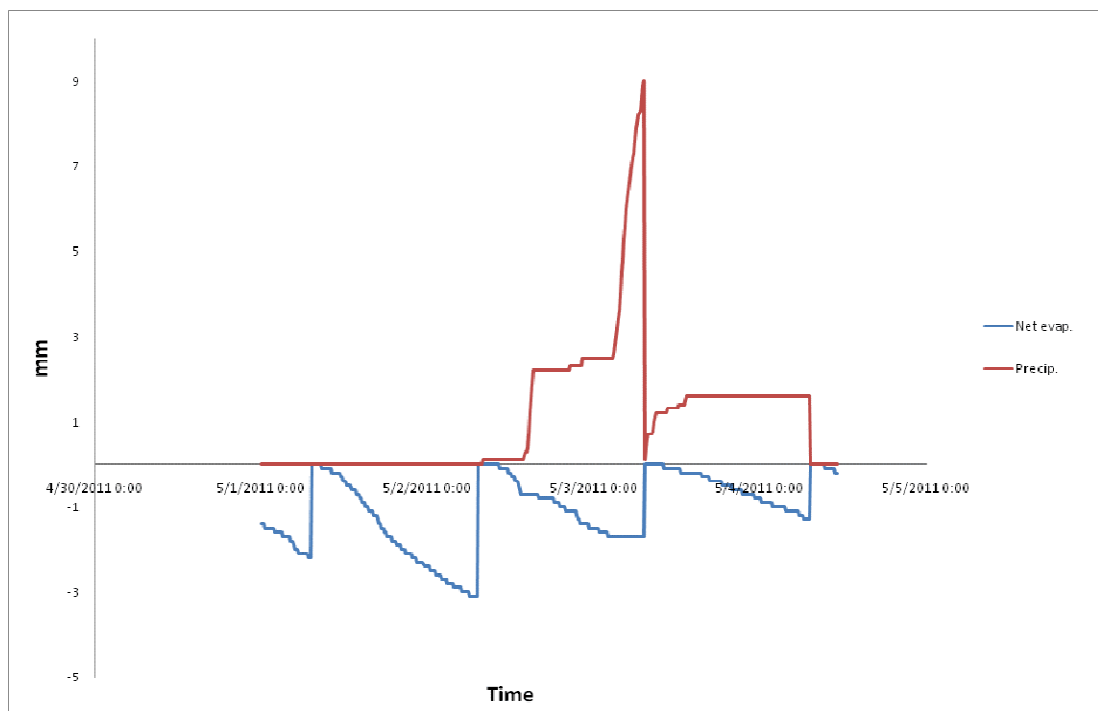


Figure 8. Estimate Net evaporation on EWM pan measurement

Compared to the results of the method “with precipitation” in Appendices 1, the result depicted in Fig. 8 is much better looking, except that it perhaps slightly underestimate the evaporation rate during the rain events.

Another task was to estimate the instantaneous evaporation rate by differentiating the net cumulative evaporation. While in reality the graph of the water level elevation is a virtually smooth curve, the graph of the net cumulative evaporation derived from the primary records was a staircase-like broken line, because the recorded water level in the pan did not change after every 10 minutes. The sensitivity of the water level sensor (0.1 mm) was not sufficient for this purpose. A numerical algorithm was developed in Excel to identify the edges of individual stairs, i.e., the instants after which the net cumulative evaporation changed. The edges of consecutive stairs were connected with a broken straight line, which represented a continuous, albeit not smooth, approximation of the net cumulative evaporation. The continuously changing values of the net cumulative evaporation could then be calculated from this broken line at any instant of time, e. g. at hourly intervals. For each such interval, an average evaporation rate was calculated as the per-interval change in the net cumulative evaporation divided by the length of the interval (e.g., one hour). A graph of the average hourly evaporation rates for May 2011 is presented in Appendix 4

Although the basic dynamics of the diurnal pan evaporation rate is discernible from the graph in Appendix 4, the graphs is still too much variable and erratic. At some hours of the afternoon, the evaporation rates are very high (up to about 10 mm d^{-1}), while at morning hours, after the restart, the rates fall to zero. The latter effect is probably caused or at least enhanced by the hysteresis of the water level sensor.

Similar evaporation rate calculations were then repeated for 3-hour (Fig. 9), 6-hour (Fig. 10) and daily (Fig. 11) intervals. It was found that the 6-hour intervals are the shortest intervals for which the resulting curve of evaporation rates is smooth enough. Fig. 14 shows the average 6-hour evaporation rates for the 2010 season. It is important to note that the vertical axes in all graphs of this type are plotted in the same units, namely, mm d^{-1} .

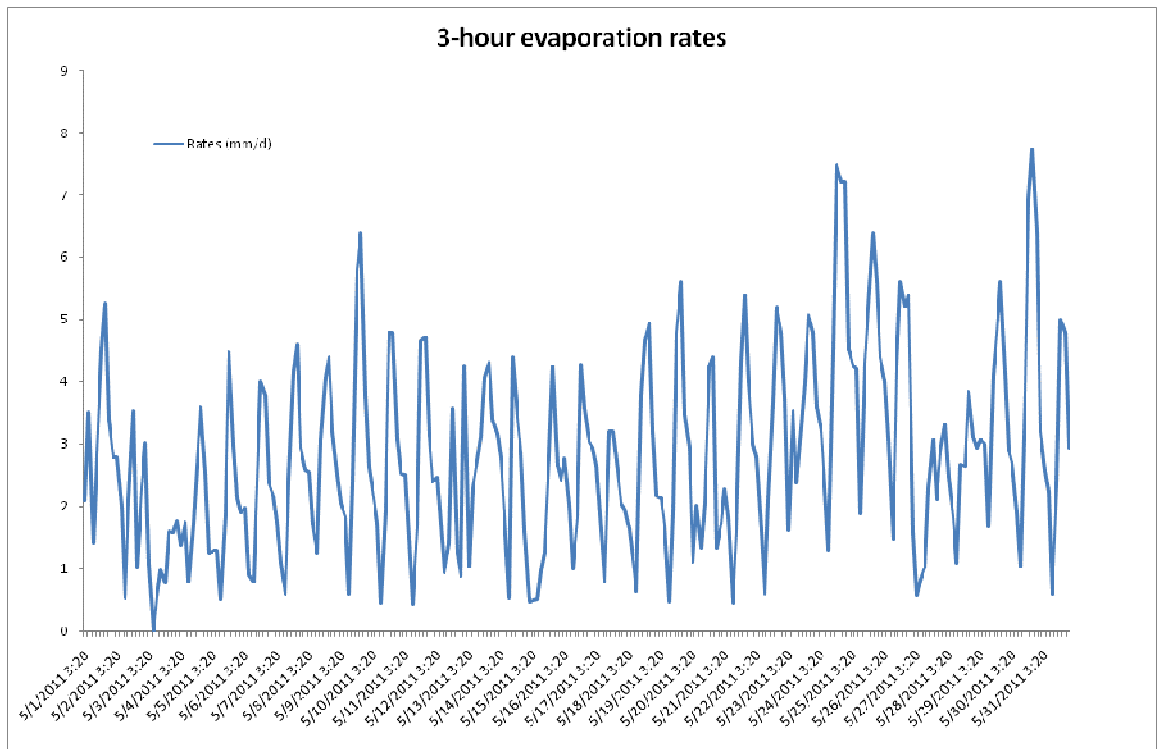


Figure 9. 3-hour evaporation rates for May 2011

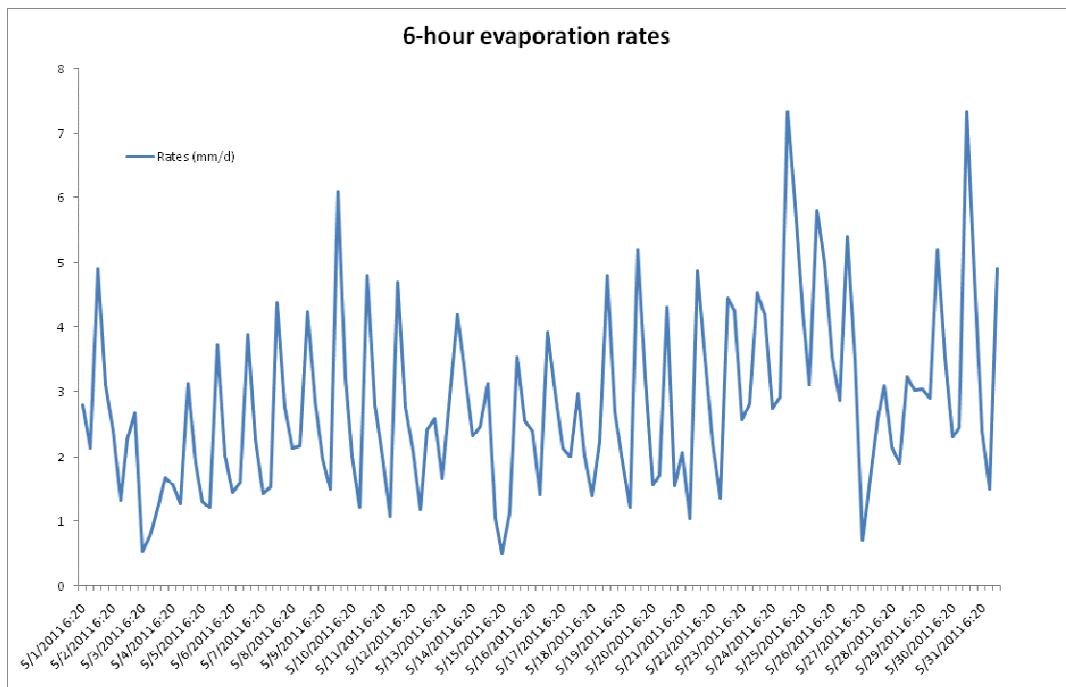


Figure 10. The 6-hour evaporation rates for May 2011

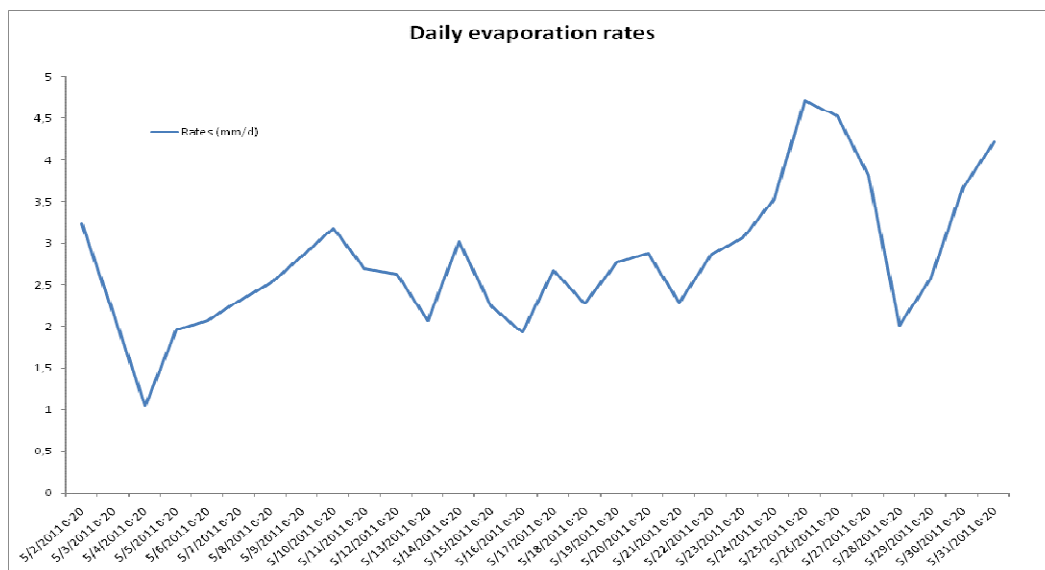


Figure 11. Daily evaporation rates for May 2011

In this way, it was demonstrated that the net water surface evaporation can be solely derived from the EWM pan measurement. In order to verify that these results are reliable, it was necessary to compare them with results obtained by the method “with precipitation”. The UFA precipitation data were compared with the data of other weather stations in the vicinity, especially with the station of the Department of Agroecology and Biometeorology of the Faculty of Agrobiological, Food and Natural Resources in the other part of the CULS campus. It was concluded that the most appropriate coefficient to multiply the UFA precipitation lies near the ratio 5:3. After this correction, the method “with precipitation” became relatively satisfactory but was only applied to daily intervals. Figure 12 and the Appendices 7 and 8 show the average daily evaporation rates for the years 2010, 2011 and 2012, respectively, estimated by the two methods, i.e. “without precipitation” (“without UFA data”) and “with precipitation” (“with UFA data”).

The agreement between the two methods are good on some days but worse on other days. The values obtained “with precipitation” show higher variability (larger differences between extremes). This can be explained by large differences between the daily precipitation sums recorded by the UFA raingauge and the EWM pan. Figure 13 and Appendices 5 and 6 compare the daily precipitation sums measured by UFA raingauge and the EWM pan for the years 2010, 2011 and 2012, respectively. The method of estimated the EWM precipitation sum is explained below. On some days, the UFA raingauge recorded high precipitation, while the pan did not show

any or only a negligible water level rise during the same day. For the days when EWM pan resulted in higher values, the data were re-checked carefully, and the cause of the discrepancy was figured out: the situation on these days was opposite to the cases mentioned above. The UFA raingauge did not record precipitation while water level in pan rose.

For instance, on 8/27/2010 a large discrepancy between the two methods occurred (Figure 13), and the primary data, starting from midnight time, were as follows:

Table 1. Details of EWM pan and UFA raingauge measurements

Time	EWM pan	UFA raingauge
8/27/2010 1:50	-0.4	0
8/27/2010 2:00	-0.2	0.5
8/27/2010 2:10	0	0.3333333
8/27/2010 2:20	0	1.1666667
8/27/2010 2:30	0	0.5
8/27/2010 2:40	0	0.6666667
8/27/2010 2:50	0	1
8/27/2010 3:00	0	0
8/27/2010 3:10	0	0
8/27/2010 3:20	0	0.3333333
8/27/2010 3:30	0	1.3333333
8/27/2010 3:40	0	1.1666667
8/27/2010 3:50	0	0.6666667
8/27/2010 4:00	0	0.1666667
8/27/2010 4:10	0	0
8/27/2010 4:20	0	5.1666667
8/27/2010 4:30	0	2.1666667
8/27/2010 4:40	0	1
8/27/2010 4:50	0	0.5
8/27/2010 5:00	0	0
8/27/2010 5:10	0	0.1666667
8/27/2010 5:20	0	0
8/27/2010 5:30	0	0
8/27/2010 5:40	0	0
8/27/2010 5:50	0	0
8/27/2010 6:00	0	0
8/27/2010 6:10	0	0
8/27/2010 6:20	0	0
8/27/2010 6:30	0	0
8/27/2010 6:40	0	0

8/27/2010 6:50	0	0
8/27/2010 7:00	0	0

As can be seen from the 2nd column, from 1:50 to 2:10 the EWM pan recorded precipitation approximately 0.4 mm (with evaporation neglected, which is a reasonable assumption at night time and high relative humidity). At the same time, the UFA raingauge recognized a heavy rain with the total of 16.833 mm falling continuously from 2:00 to 5:10. For the earlier part of the previous day, there was also a difference between the two measuring systems but it was not that significant. Subtracting the amount of precipitation recorded by two systems gives a difference between them 16.4333 mm, close to the difference in daily evaporation between the two methods (Figure 12).

However, for the remains of 2010 (excluding the days 11/8 and 11/9/2010), the daily evaporation rates with and without the UFA raingauge data fitted well to each other. The estimation of precipitation based on the EWM pan was made with the assumption that within a 10-minute interval, during which precipitation made the water level increase, there was no evaporation, which is the same calculation principle as that underlying the net evaporation calculation above, except that now only the positive changes of water level were considered. Then, this rough estimation of daily precipitation sums was compared with the precipitation sums measured by the UFA raingauge (Figure 13 for 2010). The UFA raingauge was not operational before 26/8/2010. Smaller precipitation events were recorded in a similar way by both systems, but heavy rain events not. Hence, increasing the amount of UFA raingauge precipitation by the coefficient of 5:3 effectively confirmed the validity of the two methods. The differences exist between the precipitation sums recorded by the two system, either due to actual rainfall heterogeneity or due to some unrecognized errors in measurement, rather than between the two methods of data processing, which on average, give the same results.

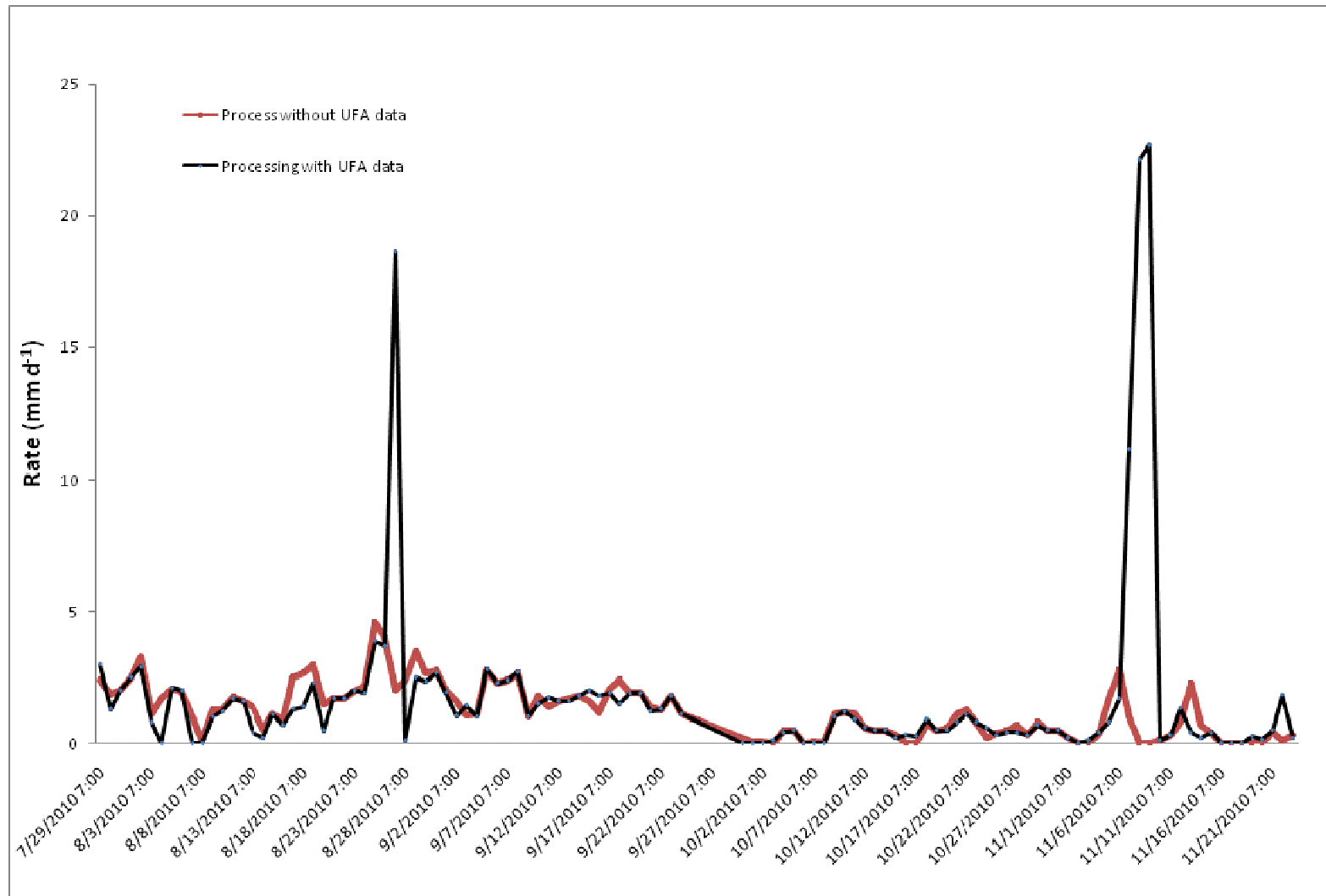


Figure 12. Comparison between the two methods of processing EWM pan measurement, year 2010

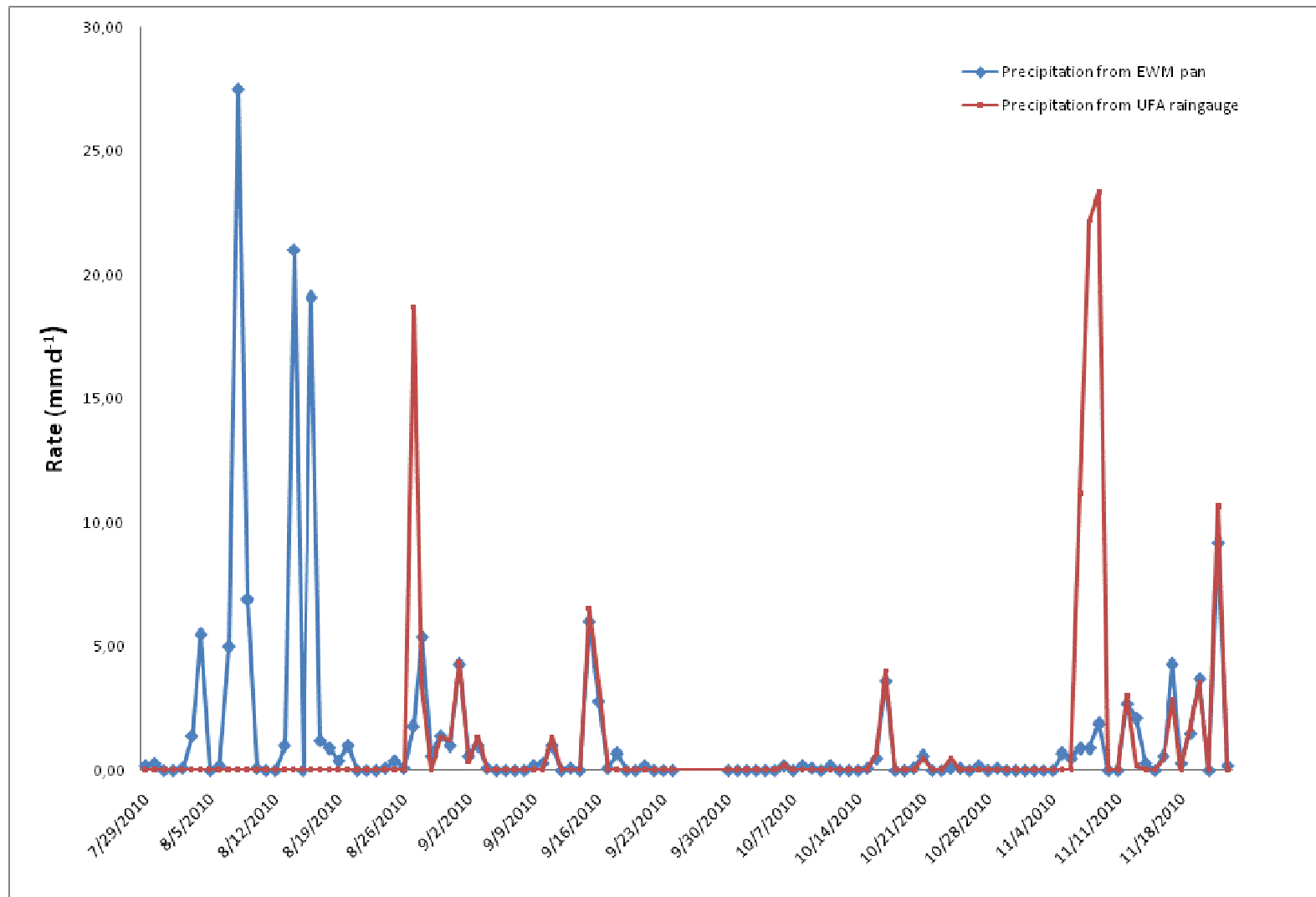


Figure 13. Rough estimation of precipitation obtained from EWM pan and UFA raingauge, year 2010

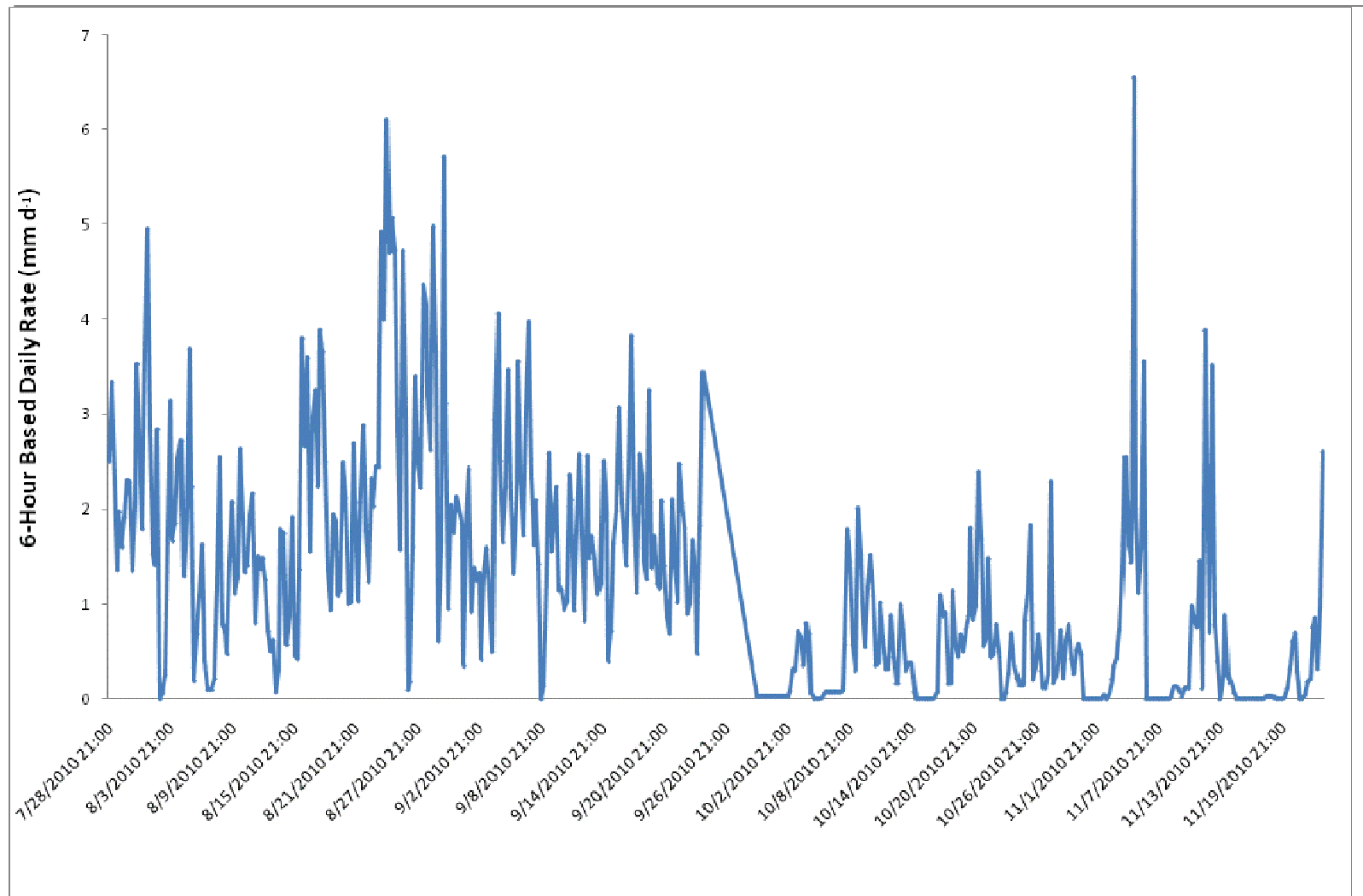


Figure 14. The 6-hour evaporation rates - 2010

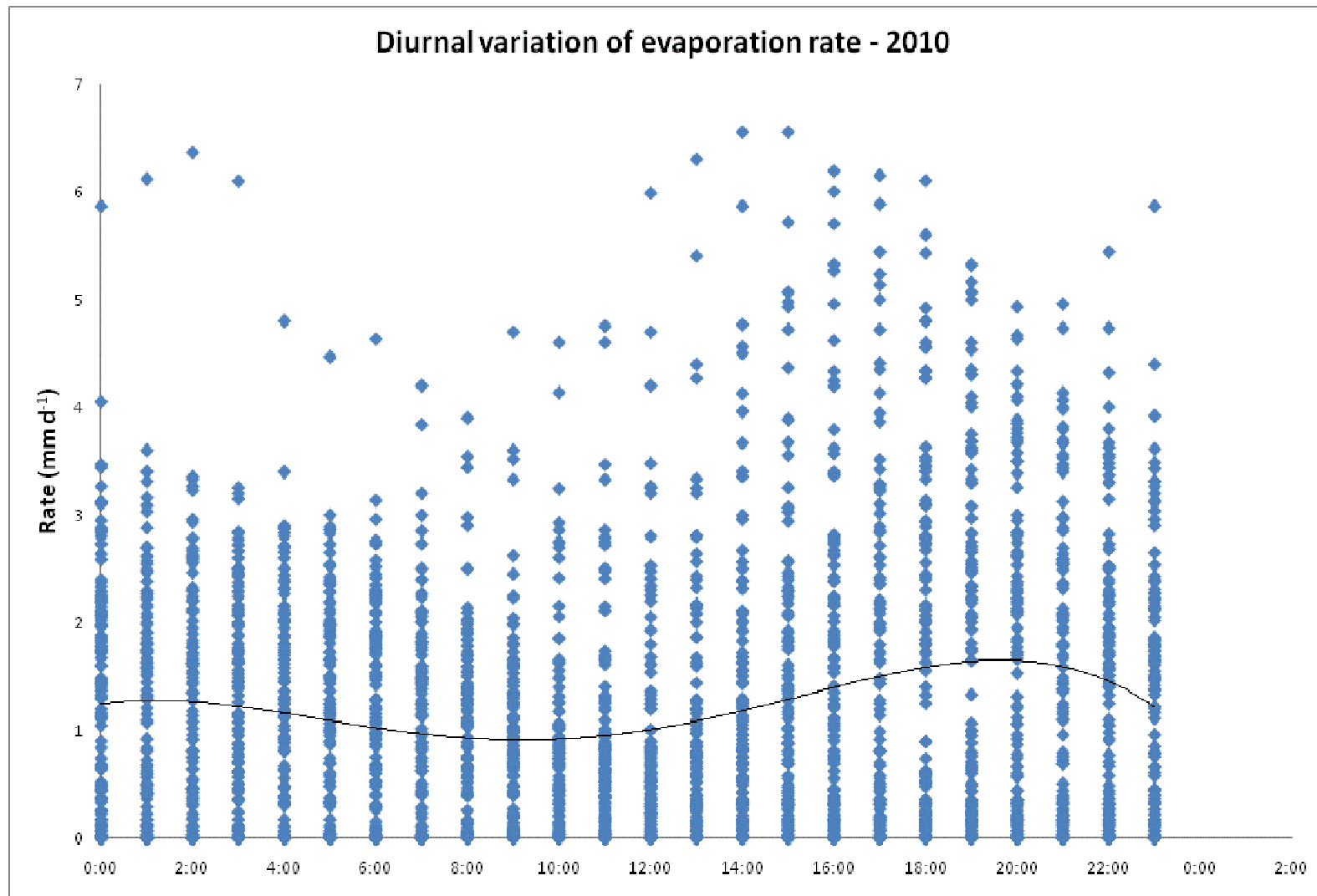


Figure 15. Diurnal variation of evaporation rate - 2010

As soon as we start to investigate the diurnal variation of evaporation rate, it may be insufficient to do it only for four different time instants in each day. Fig. 15 shows the plot of 6-hour daily evaporation rates calculated as moving averages for each hour of the day (this hour being the center of the 6-hour interval). Since the average 6-hour evaporation rates create a relative smooth curve, they suit our purpose to clarify the typical diurnal fluctuation pattern of the evaporation rate. In Fig. 15, there is only the hour of the day plotted on the horizontal axis, which gives us an opportunity to explore a diurnal variation pattern typical for the entire season. A polynomial function was employed to fit the data and to indicate the probable position of the maximum and minimum evaporation rates. A well-defined minimum occurs at about 19:00, while the lowest evaporation rate is observed at about 9:00. Each morning the evaporation rate gradually increases from 9:00 until about 19:00 and then falls down again.

This diurnal pattern can be explained as the water in pan is being heated up during the day, and stores this long into the evening which keeps it from responding immediately to the falling temperature of the atmosphere. The difference between the saturated vapor pressure at the water surface temperature and the actual water vapor pressure in the air becomes maximal in the evening, which brings about the evening maximum of evaporation rate, in accordance with the Dalton law (2).

Similar trends were obtained for the diurnal variation for the years 2011 and 2012 (see Appendices 9 and 10).

5.2. Dalton's equation for potential evaporation

Dalton used only two state variables to depict potential evaporation. As both the saturated vapor pressure of water surface and the actual vapor pressure in the air were known in our case, it was possible to find the turbulent exchange function $f(u,z)$ in Dalton's equation (2). Also the turbulent exchange function (wind function) used in Penman's equation was estimated according to Calder's form of the Penman formula(39).

Fig. 15 shows the Dalton and the Penman wind functions for the 2011 season. To some extent, the Dalton turbulent exchange function behaves similarly to the Penman wind function, but is in most instances smaller. At some points the Dalton's function fall to zero when the EWM pan did not record any evaporation. On 26/10/2011, an extremely high value of Dalton's function was obtained, exceeding 3 times the Penman's. The explanation for this extreme is that weather on this day was humid, so that the saturated vapor pressure at water surface temperature and the actual vapor pressure were not significantly different.

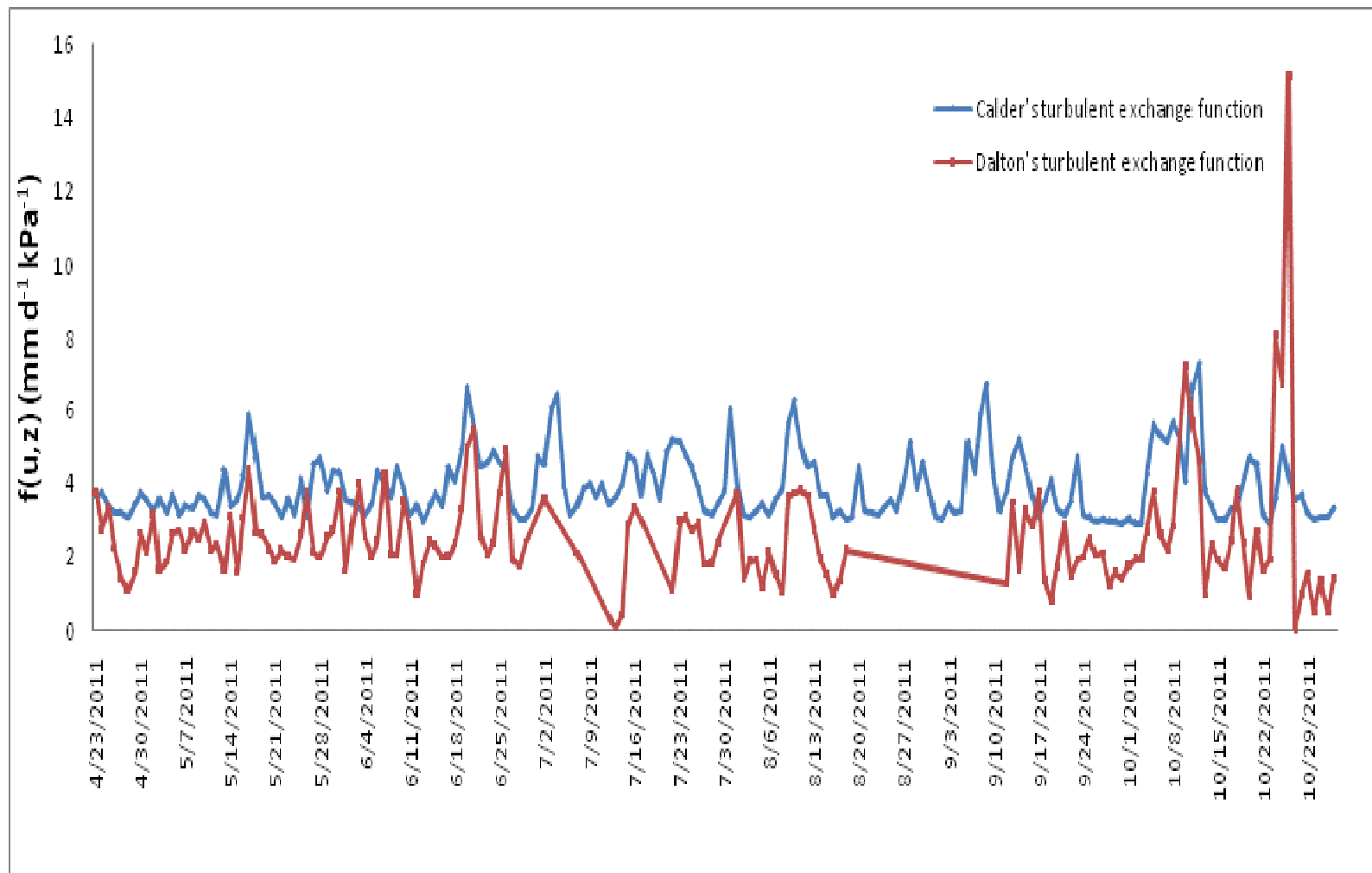


Figure 16. Turbulent exchange function - 2011

5.3. Penman's equation for potential evaporation

Following the procedures recommended in the FAO 56 documentation (Allen et al., 1998) and overviewed in previous sections, several important solar radiation components were computed for the periods of investigation, while the downward short-wave solar radiation R_{sd} was measured. The net radiation values for water $R_{n,w}$ and for soil covered with grass $R_{n,s}$ were computed by applying different albedo.

The albedo value for water was taken as 0.08, while that for the grass was taken as 0.23. Adopting albedo 0.08 in the Penman equation (6) results in high potential evaporation values, exceeding the EWM pan measurement, with larger difference in summer months (from April to Mid of September), while in autumn months (September and October) the two data sets were to a greater extent similar (in winter months the pan evaporation was not measured). A reasonable explanation of the discrepancy might be the neglect of soil (water) heat flux term in the Penman equation. In summer time, the amount of heat transfer to the Earth subsurface would be greater than in other seasons. As a consequence, the radiation term in Penman equation in fact contains an overestimated energy supply rate, especially in summer months. Moreover, as pointed out by Mekonnen et al. (2012), the reflective characteristic of the metallic pan or unaccounted effect of water stratification due to mixing and conduction (Mekonnen, 2012, Martinez, 2005) may act in the same direction.

Hence, the optimization of albedo was done for two different periods, corresponding to this argument. The pan measurement was taken as the potential evaporation in the Penman formula, then the corresponding net radiation was found out, because all other terms in Penman's equation were fixed known either from measurements or from reliable empirical formulae. An optimized value of albedo was estimated from the new value of net radiation, representing all the effect mentioned above, i.e. the seasonal fluctuation of soil and water heat flux and the actual reflectivity of the EWM water pan.

For summer time, an optimized value of albedo was 0.3486, while for autumn time it remained at 0.08. Details graphs of the optimization results are presented in Appendices 11 and 12.

The potential evaporation was also calculated according to the a simplified formula (16) proposed by Valiantzas. Values of albedo was set similar to the value applied above in Penman original formula. However, the turbulent exchange function was kept as Valiantzas suggested. It

equaled $0.5 + 0.536 * u_2$ instead of the original Penman (39). Fig. 17 offers a comparison of the EWM daily evaporation sums for 2011 with the values obtained by the Penman equation with the albedo optimized and by the Valiantzas (simplified Penman) equation (16). Analogous graphs for 2010 and 2012 can be found in Appendices 13 and 14. The year 2011 was chosen for being placed in the main text (Fig. 17), because the seasonal variation is better visible there than in the incomplete season 2010.

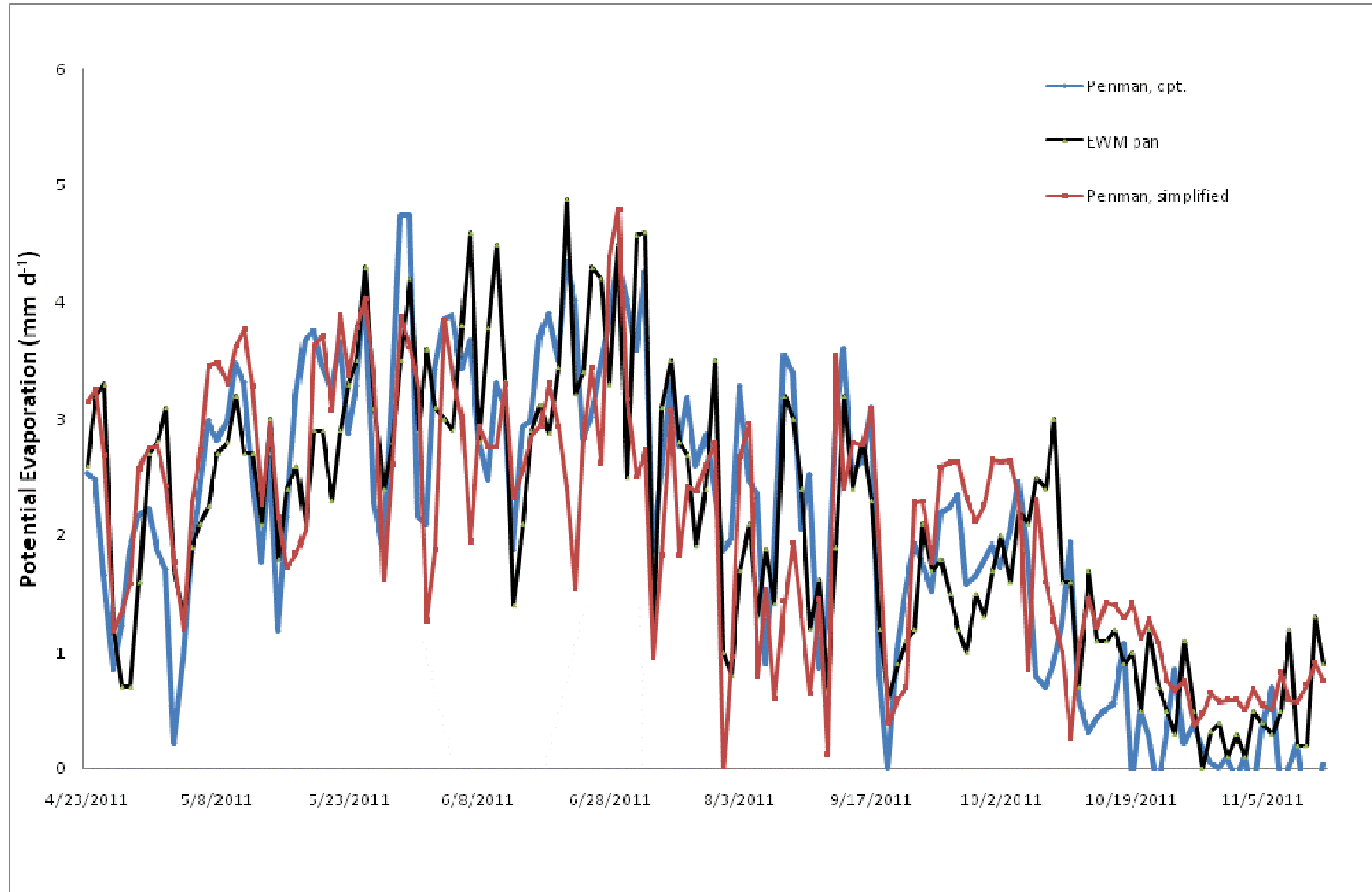


Figure 17. Comparison of different methods of estimating potential evaporation

Fig. 17 shows that the general seasonal trend is similar for the EWM pan measurement as well as the Penman equation and the simplified Penman. The annual variation of evaporation rates corresponds to what one would expect: the highest rate of evaporation occurs in summer and gradually decreases in autumn. The evaporation rates in winter and spring are also expected to be lower than those in summer, mainly as a result of low net radiation.

The Penman equation and the EWM pan measurements are in satisfactory accordance with each other. The Penman evaporation rates are a little higher than the EWM pan rates, with some exceptions: on the days with precipitation events, we would expect that the actual vapour pressure in the air could exceed the saturation vapour pressure at the water surface which, together with small net radiation, would lead to low evaporation rates. However, the EWM pan keeps evaporating at high rates even on these days. This could be considered as inaccuracy of the pan itself.

The simplified Penman procedure usually underestimates the evaporation in the middle of the season and underestimates it at the beginning and end of the season.

Let us clarify in a greater detail which conditions may cause the divergence between the three methods. For example, one unexpected event occurred on 26/8/2010, when EWM pan and the Penman equation provided approximately same estimation of potential evaporation, while the simplified Penman value is low. The difference in wind functions applied was small. Regarding the simplified Penman equation, it included several meteorological parameters of which some are similar to those used in the Penman equation. However, the simplified Penman equation depends on the value of average temperature in a subtracted term. On this day, average temperature was higher than on days with similar maximal and minimal temperatures, leading to a decrease in potential evaporation estimated by the simplified Penman.

There was also an unexpected difference between the Penman equation and the EWM pan on 11/9/2010. For this day, the temperature of water surface was not diverge much from the average air temperature, the wind speed was also low and, according to Dalton theory, the potential evaporation was small. However, the corresponding Penman formulae (both the original and the simplified one) involve the vapor pressure deficit which was still large on this day, leading to a high value of estimated evaporation. Similar explanation also pertains with respect to the FAO 56 reference crop evapotranspiration (see below).

5.4. FAO 56 Penman-Monteith equation for reference crop evapotranspiration

Substituting all measured or otherwise determined weather elements into (15) gives the FAO 56 values of the reference crop evapotranspiration. This was done with the daily weather data measured on the experimental site in the seasons 2010-2012. The results were compared with daily sums of the EWM pan evaporation. It follows from the comparison (Fig. 18) that the reference crop evapotranspiration (ET_0) is almost considerably lower than the pan evaporation (E_{pan}). It was a theoretical expectation anyway, but the average ratio of ET_0 to E_{pan} (the pan coefficient k_{pan}) was 0.44, considerably lower than the recommended range 0.6 - 0.8 (Allen et al., 1998).

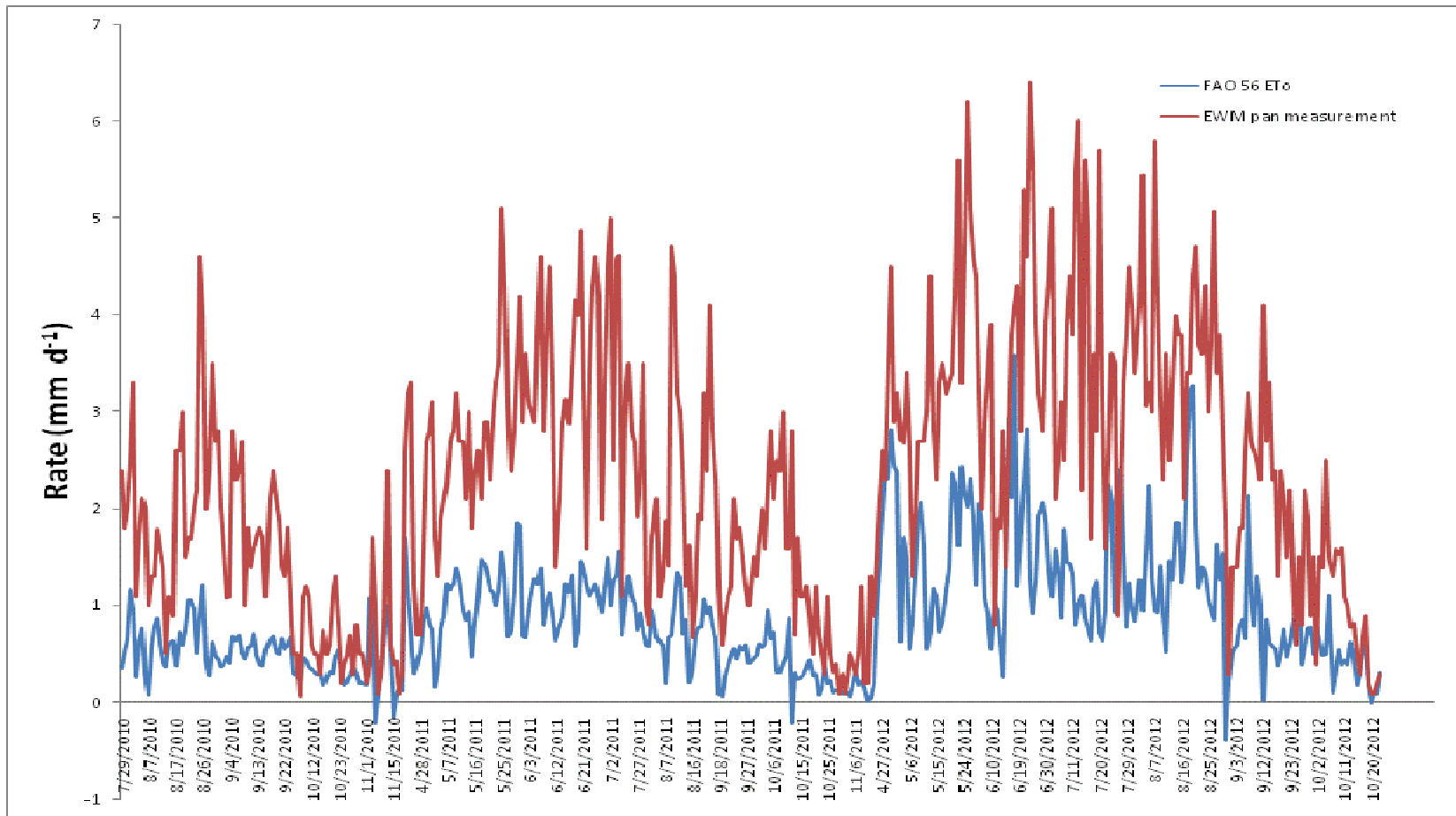


Figure 18. FAO 56 Evapotranspiration and EWM pan measurement, 2010-2012

6. Discussion

The data collected in the experimental field of the Department of Water Resources, Faculty of Agrobilogy, Food and Natural Resources, Czech University of Life Sciences, Prague, were used to estimate the potential (open water surface) evaporation. The methods involved were: pan measurement and Penman-type equations. The potential evaporation was obtained from the EWM pan measurement. Two methods of pan data processing were used, one combining the pan data with precipitation data of the UFA tipping bucket raingauge, the other one solely based on the pan data. Theoretically the two methods may perfectly fit to each other, as the water level in the EWM pan rose due to precipitation and fell due to evaporation. However, the actual results of data processing with and without precipitation data were not exactly the same. Hence, it was necessary to check backwards the compatibility between two measurement equipments. By comparison to the data from another CULS' weather station, it was found that the UFA raingauge underestimated precipitation events, as the ratio between UFA data and the other station's data was approximately 3:5. To deal with this problem, a coefficient 5:3 was used to multiply all original UFA precipitation data. Then the net evaporation obtained with UFA data was better correlated to the net evaporation based solely on the EWM pan data. Nevertheless, some differences persisted, especially on days with heavy precipitation recorded by raingauge. This might be a systematic error due to incompatibility of the two measuring systems (the EWM pan and the raingauge) or spatial heterogeneity of intensive precipitation. Therefore, to avoid the propagation of errors from the raingauge data, the following analyses were based on the net evaporation relying solely on the EWM pan data.

The EWM pan data made it possible to describe, in rough terms, the fluctuation of the evaporation rate during the day and night. A polynomial trend line similar to a sine curve approximated the average pattern diurnal variation over all days of a particular season. To clarify this diurnal trend of evaporation with daily maxima and minima, twenty-four series of average 6-hour evaporation rates, each series shifted with respect to the previous one by one hour, were calculated in this way and plotted against the hour of the day in the middle of the 6-hour interval. A clear trend was figured out: On average, the maximum evaporation was reached each day at about 19:00. Then it decreased gradually and a minimum was reached at about 9:00 am. Then it started to rise again.

Using meteorological data available from the field measurements, the Penman original equation and a simplified Penman equation proposed by Valiantzas were also used to estimate the potential (water surface) evaporation. First, the recommended value of albedo for water surface, 0.08, was used, which led to an overestimated evaporation compared to the pan measurement. A larger difference was observed in summer time, while in autumn and a small part of winter (over which the EWM pan could operate) the difference was lower, as a consequence of a larger value of the neglected soil heat flux in summer, compared to the other seasons. Hence, two different values of albedo were applied. An optimized albedo, 0.3486, representing both the higher reflectivity of the pan stainless steel and the neglected soil heat flux, was used in summer (from April to September), while the low value, 0.08, was use for the rest of the time.

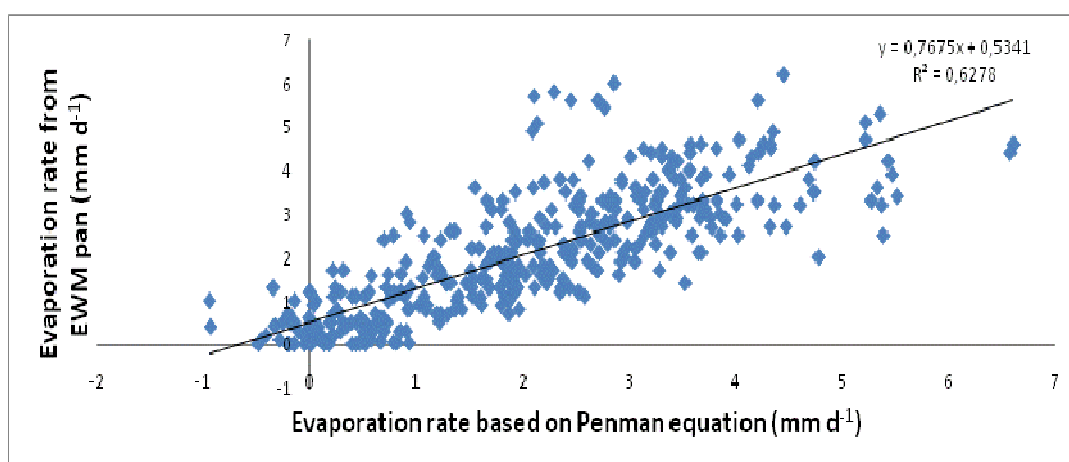


Figure 19. Correlation between EWM pan measurement and Penman equation

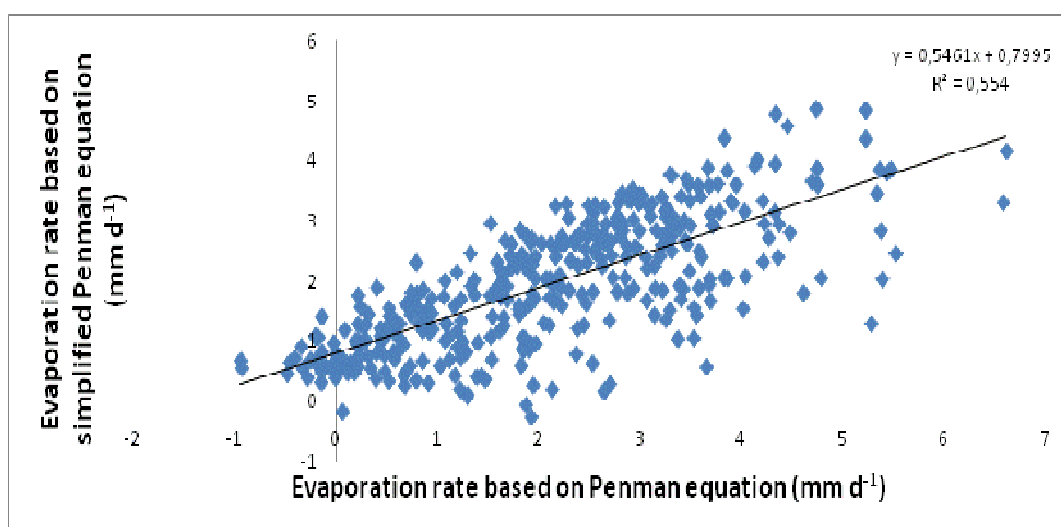


Figure 20. Correlation between simplified Penman equation and Penman equation

On some days there are large differences between the pan evaporation, the original Penman equation and the simplified Penman, an overall characterisation of correlations between these variables using the root mean squared error (RMSE) would not provide an accurate view of the correlation. Instead, the correlation was described in the form of linear regression as in the graphs above, with acceptable values of the correlation coefficient.

The FAO 56 Penman-Monteith daily values of the reference crop evapotranspiration was estimated. The pan coefficient k_{pan} was then calculated from the average ratio of the potential evaporation to the reference crop evapotranspiration, equaled 0.44. At this step, the soil heat flux was still neglected but the albedo was in the FAO 56 Penman-Monteith was not yet modified, so in summer time, the divergence between the evaporation and evapotranspiration was large, in parallel with the trend of optimized albedo for the Penman equation (see above).

In a further research on this topic, it may be better to measure the soil heat flux directly rather than including it in the value of albedo since in this research, only one value of albedo was used to characterize the soil heat flux, while in fact it changed days by days. Moreover, the accuracy of the UFA rain gauge should be revised since the pan evaporation estimates “with precipitation” and “without precipitation” are largely different on rainy days.

Although there also was a possibility to calculate monthly evaporation according to the Thornthwaite method based on the available air temperature data, the total time for which the pan measurements were available was not sufficient to make a statistical evaluation. Hence, longer observation would help determine the coefficient for the Thornthwaite formula, with the advantage of less data requirement, since only the monthly temperatures are employed there.

The simplified Penman equation gave almost equally accurate estimation of the potential evaporation as the Penman equation. However, the empirical parameters used need to be changed to adapt well with the local conditions which might require longer observation. Though there were gaps in estimation methods (in empirical parameters) and in the quality of data (such as gaps in EWM pan measurement), the Penman equation or the measurement from EWM pan could become alternative for each other. Moreover, the combination of empirical equation and pan observation if once calibrated substantially (which also require longer and more accurate observation) would help deepen the understanding on surface energy balance, thus further the knowledge on surface hydrology balance and the effect climate change on water evaporation.

7. Conclusion

The objectives of this study were to find out if and to what extent the EWM evaporation pan, the Penman equation and the Penman simplified give correct values of water surface evaporation, to elaborate an optimum method for correcting the gross evaporation data for the effect of precipitation and to explore the variation of water surface evaporation over the diurnal period and over longer time intervals. These objectives were fulfilled.

The thesis used data from the weather station belonging to the Department of Water Resources, Faculty of Agrobiological Sciences, Food and Natural Resources, Czech University of Life Sciences for estimating potential evaporation from August 2010 to November 2012 (excluding winter months). Through the processing of pan and weather data, the accuracy of the equipment (EWM pan) was checked and an incompatibility between the rain gauge and the EWM pan was discovered with a high probability of a malfunctioning of the instruments during heavy precipitation events. The net evaporation was from the EWM pan, its diurnal variation was estimated and also its seasonal variation (in a simplified manner). Two Penman-type equations based on the combination method were evaluated using weather data from the experimental site. The evaluation and comparison were done with both the original and the optimized albedo. In the case of using the recommended albedo of 0.08, the Penman equation and the simplified one both overestimated significantly the potential evaporation in summer time but not so much in other seasons in year. With a modified albedo, the results from the two Penman-type equations gave better estimation of net evaporation measured by EWM Pan in the summer, because the modified albedo included the effect of larger soil heat flux in summer. Although better results were gained with the modified albedo, some differences still about its accurate value. Thus, it is better to conduct separate measurement of soil heat flux than to neglect it altogether and include its effect in an average albedo for the whole season. Last but not least, I included a calculation of the reference crop evapotranspiration for the same weather condition, aiming to find a pan coefficient for conversion from the EWM pan evaporation and the reference crop evapotranspiration. A value of 0.44 was found, although it was lower than the recommended range from 0.6 to 0.8.

Bibliography

Allen, R.G., Pereira, L.S., Raes, D., Smith, M. 1998. Crop evapotranspiration: Guidelines for computing crop water requirements. FAO Irrigation and Drainage Paper, No. 56. FAO. Rome. p. 300. ISBN 92-5-304219-2.

Bouchet, R. J., 1963. Evapotranspiration réelle et potentielle, signification climatique. Proc. IASH General Assembly, Berkely, CA, Special Publication Vol. 62. International Association of Scientific Hydrology. p. 134–142.

Brutsaert, W., Stricker, H. 1979. An advection-aridity approach to estimate actual regional evapotranspiration. *Water Resources Research* 15(2). 443-450.

Chen, D., Gao, G., Xu, C. Y., Guo, J., Ren, G. 2006. Comparison of the Thornthwaite method and pan data with the standard Penman-Monteith estimate of reference evapotranspiration in China. *Climate Research*. Vol. 28. 123 – 132.

Chow, Ven Te 1964. *Handbook of Applied Hydrology: A Compendium of Water Resources Technology*., McGraw Hill, p. 1450. ISBN-10: 0070108102

Cobaner, M. 2013. Reference evapotranspiration based on Class A pan evaporation via wavelet regression technique. *Irrigation Science*, 31. 119 - 134.

Crago, R., Crowley, R. 2005: Complementary relationships for near-instantaneous evapotranspiration. *Journal of Hydrology* 300. 199-211.

Dolezal, F. 1994. Lecture notes on Transport of water in soil-plant-atmosphere continuum. National University of Ireland, Galway, Ireland.

Doorenbos, J., Pruitt, W. O. 1977. Crop water requirements. FAO Irrigation and Drainage Paper No. 24, FAO. Rome.

FAO. Reference Manual. 2012. ver. 3.2: Evaporation from a reference surface. FAO, Rome

Gash, J. H. C., Shuttleworth, W. J. 2007. Evaporation / Selection, introduction and commentary. International Association of Hydrological Sciences. Benchmark papers in hydrology. ver. 2.

Hargreaves, G. H., Samani, Z. A. 1982. Estimation of Potential Evapotranspiration. Journal of the Irrigation and Drainage Division, Proceedings of the American Society of Civil Engineers. 108 (3). 225-230.

Hargreaves, G.H., Samani, Z.A. 1985. Reference crop evapotranspiration from temperature. Applied Engineering in Agriculture 1(2). 96-99.

Jensen, M.E. 2010. Estimating evaporation from water surface. CSU/ARS Evapotranspiration Workshop, Fort Collins, CO.

Keskin, M.E., Terzi, O., Taylan, D. 2004. Fuzzy logic model approaches to daily pan evaporation estimation in western Turkey. Hydrological Sciences Journal. 49:6.-1010.

Knozova, G., Roznovsky, J. , Kohut, M. 2005. Comparison of evaporation time series measured by evaporimeter GGI 3000 and that calculated by the FAO method. (In Czech). Bioklimatologie soucasnosti a budoucnosti.

Martinez, J.M.M., Alvarez, V. M, Gonzalez-Real, M. M, Baille, A. 2005. A simulation model for predicting hourly pan evaporation from meteorological data. Journal of Hydrology 318. 250 – 261.

Mekonnen, G. B., Dolezal, F., Matula, S. 2012. Using the Dirichlet boundary condition for soil evaporation at all times. Private communication.

Monteith, J.L. (1965). Evaporation and environment. Symp. Soc. Exp. Biol. 19, 205-224.

Monteith, J.L., Unsworth, M.H. 1990. Principles of environmental physics. Second edition. Edward Arnold, London, p. 291. ISBN: 9780713129311

Morton, F.I. 1983. Operational estimates of areal evapotranspiration and their significance to the science and practice of hydrology. Journal of Hydrology 66: 1-76.

Penman, H.L. 1948. Natural evapotranspiration from open water, bare soil and grass. Proceedings of the Royal Society of London. Series A, 193. 120–146.

Priestley, C.H.B., Taylor, R. J. 1972. On the assessment of surface heat flux and evaporation using large-scale parameters. *Mon. Weather Rev.*, 100. 81-82.

Ramirez, J.A., Hobbins, M. T. 2005. Observational evidence of the complementary relationship in regional evaporation lends strong support for Bouchet's hypothesis, *Geophysical research letters*. Vol. 32, L15401.

Stull, R. 2011. Wet bulb Temperature from Relative Humidity and Air Temperature. *Journal of Applied meteorology and climatology*. Vol. 50. 2267 - 2269.

Thornthwaite, C.W. 1948. An approach toward a rational classification of climate. *Geographical Review* 38(1): 55-94.

Valiantzas, J.D. 2006. Simplified versions for the Penman evaporation equation using routine weather data. *Journal of Hydrology* 331, 690 - 702.

Xu, C. Y., Singh, V. P. 2001. Evaluation and generalization of temperature-based methods for calculating evaporation. *Hydrological processes*. 15, 305-319.

Wilson, G. W, Fredlund, D. G., Barbour, S. L. 1997. The effect of soil suction on evaporative fluxes from soil surface. *Canadian Geotechnical Journal*. 34(4). 145-155.

WMO. Guide to meteorological instruments and methods of observation, 2008, 7th edition. World Meteorological Organization. Switzerland. p. 681. ISBN 978-92-63-10008-5.

Other information sources:

Historical weather data in Prague. Online database of Czech Meteorological Institute. http://www.chmi.cz/portal/dt?portal_lang=en&menu=JSPTabContainer/P3_0_Informace_pro_Vas/P3_9_Historicka_data&last=false, accessed online 20th March 2013.

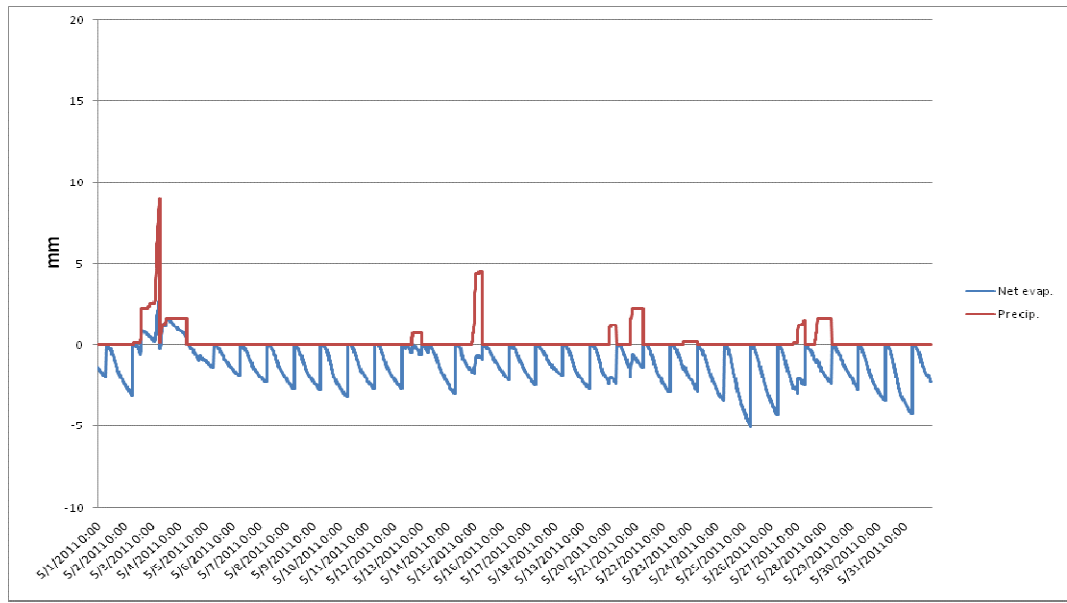
Lecture on

Evapotranspiration. <http://search.boisestate.edu/?q=evapotranspiration&site=boisestate.edu>, accessed online 20th March, 2013.

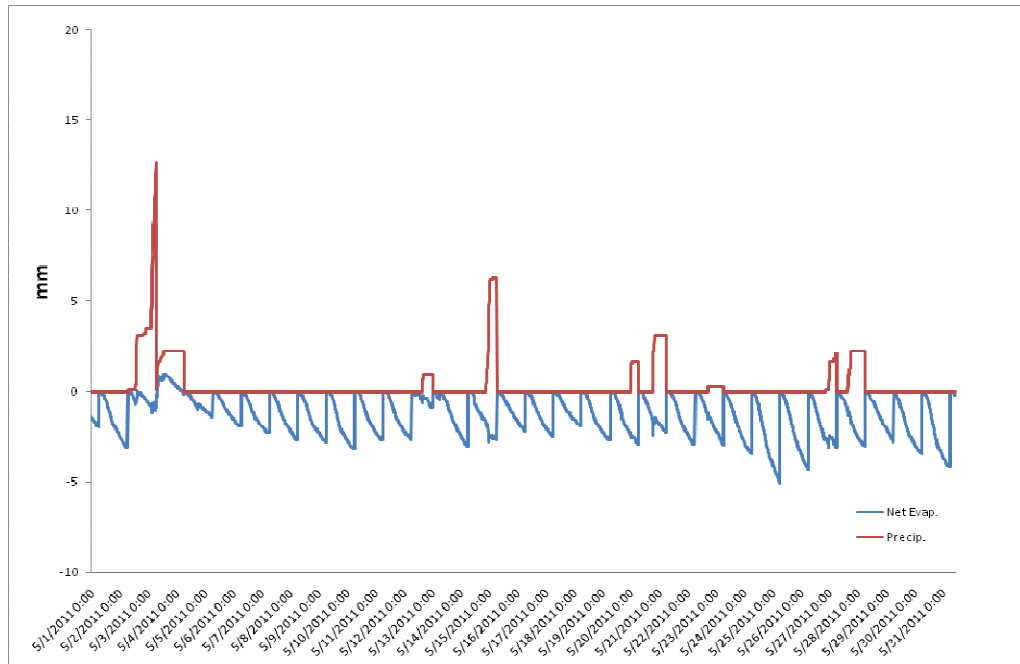
Measurement and Processing of Meteorological Data. Online database, Indian Institute of Technology Madras, <http://nptel.iitm.ac.in/courses/105107129/module5/lecture1/lecture1.pdf>, accessed online 26th March 2013.

Appendix

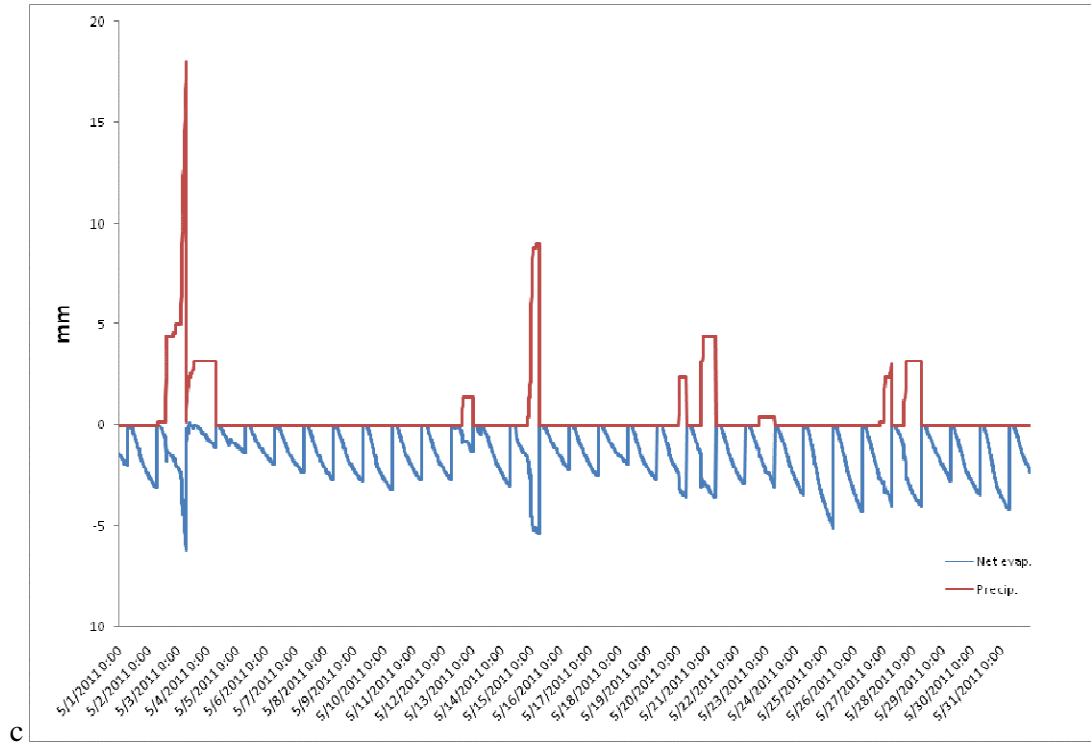
Appendix 1: Graph on primary calculation Net evaporation = Water level in pan - Cumulative Precipitation



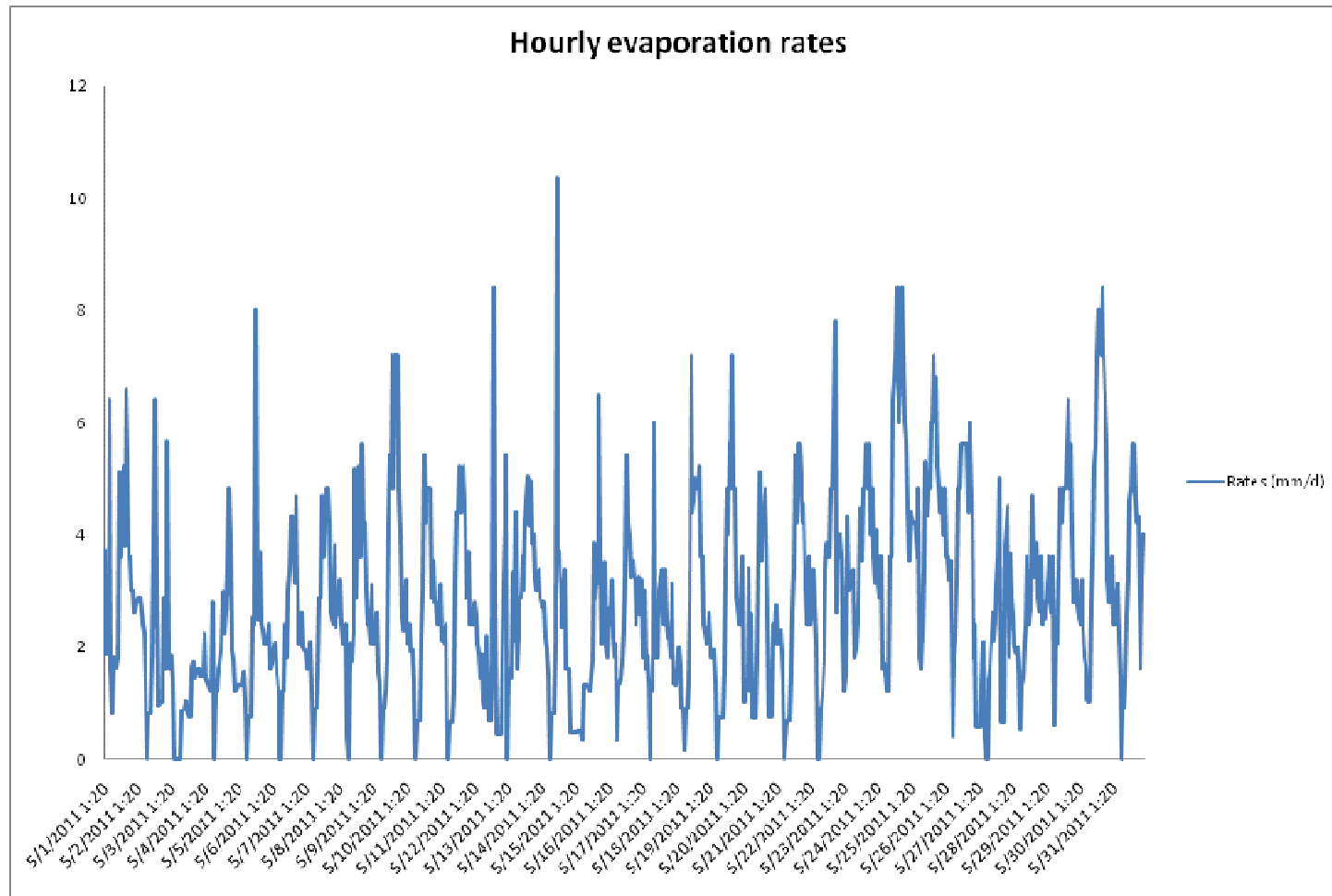
Appendix 2. Net evaporation = Water level in pan - Cumulative precipitation * 1.4



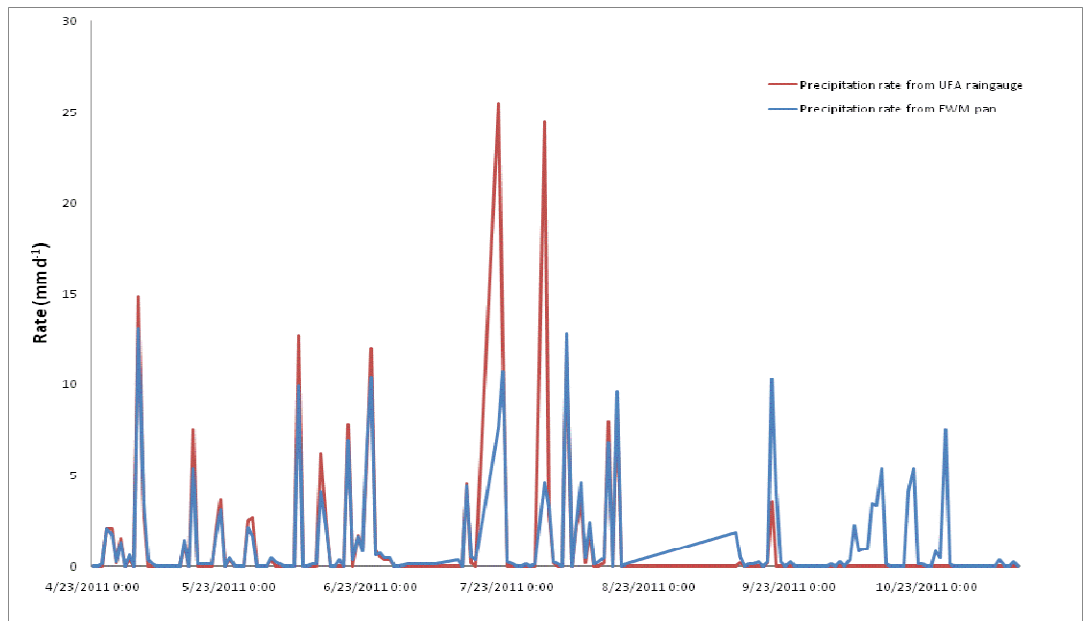
Appendix 3. Net evaporation = Water level in pan – Cumulative precipitation * 2



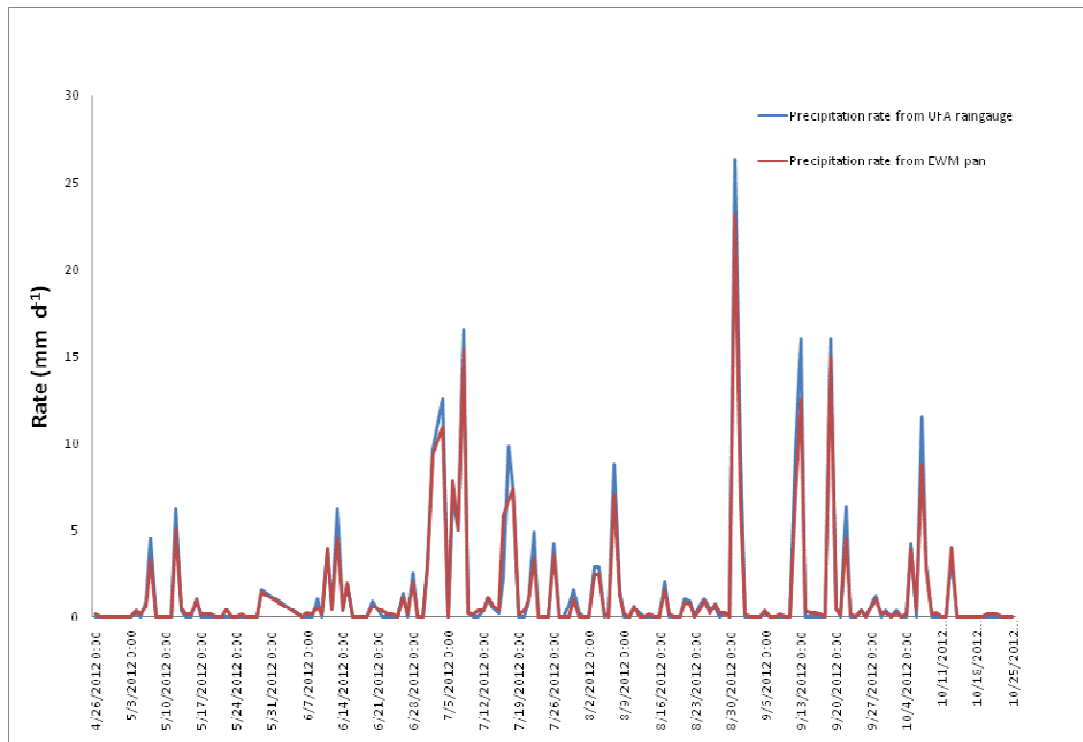
Appendix 4. Daily evaporation rate based on hourly sum



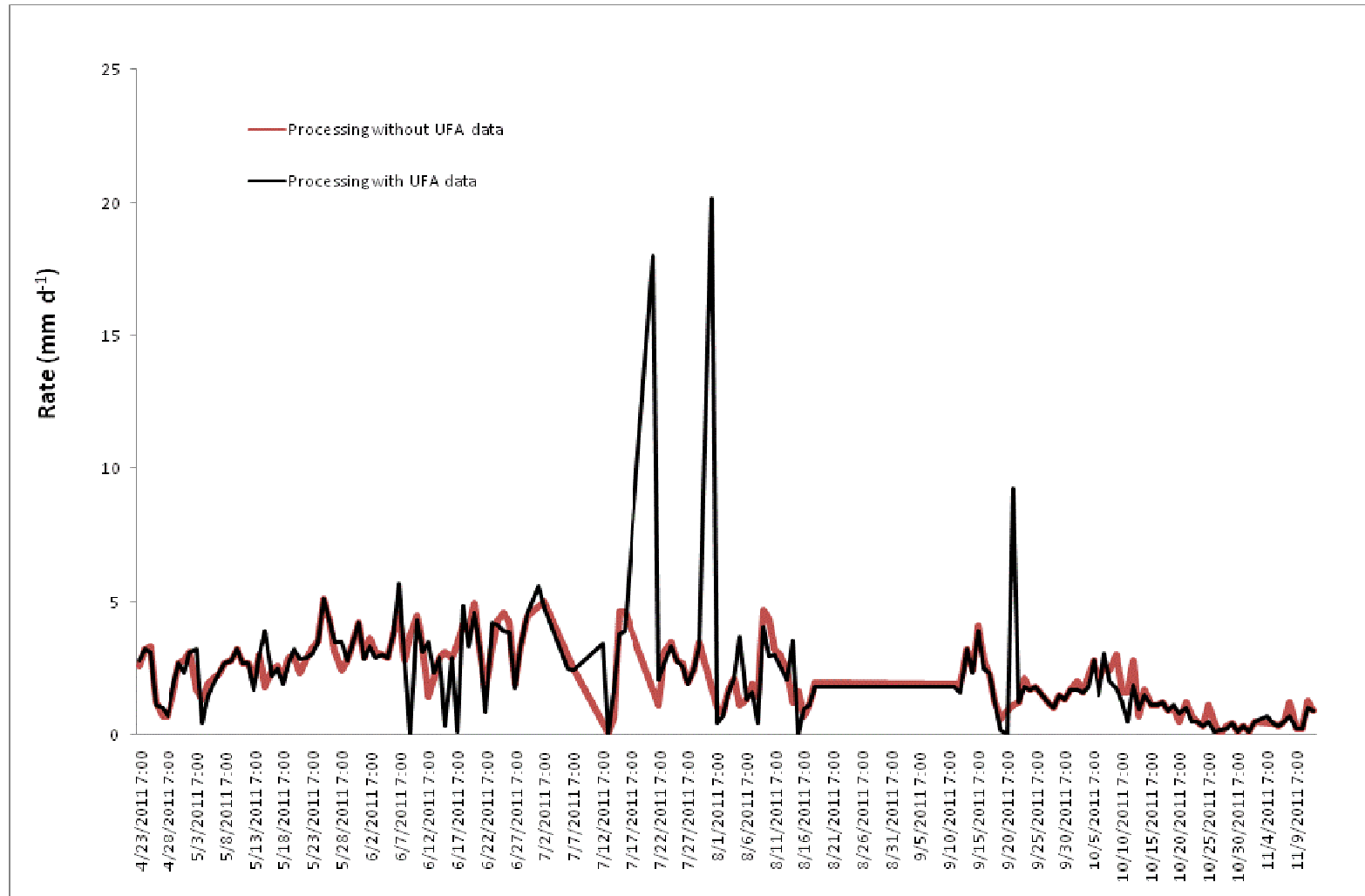
Appendix 5. Estimation of precipitation from EWM pan and UFA raingauge, year 2011



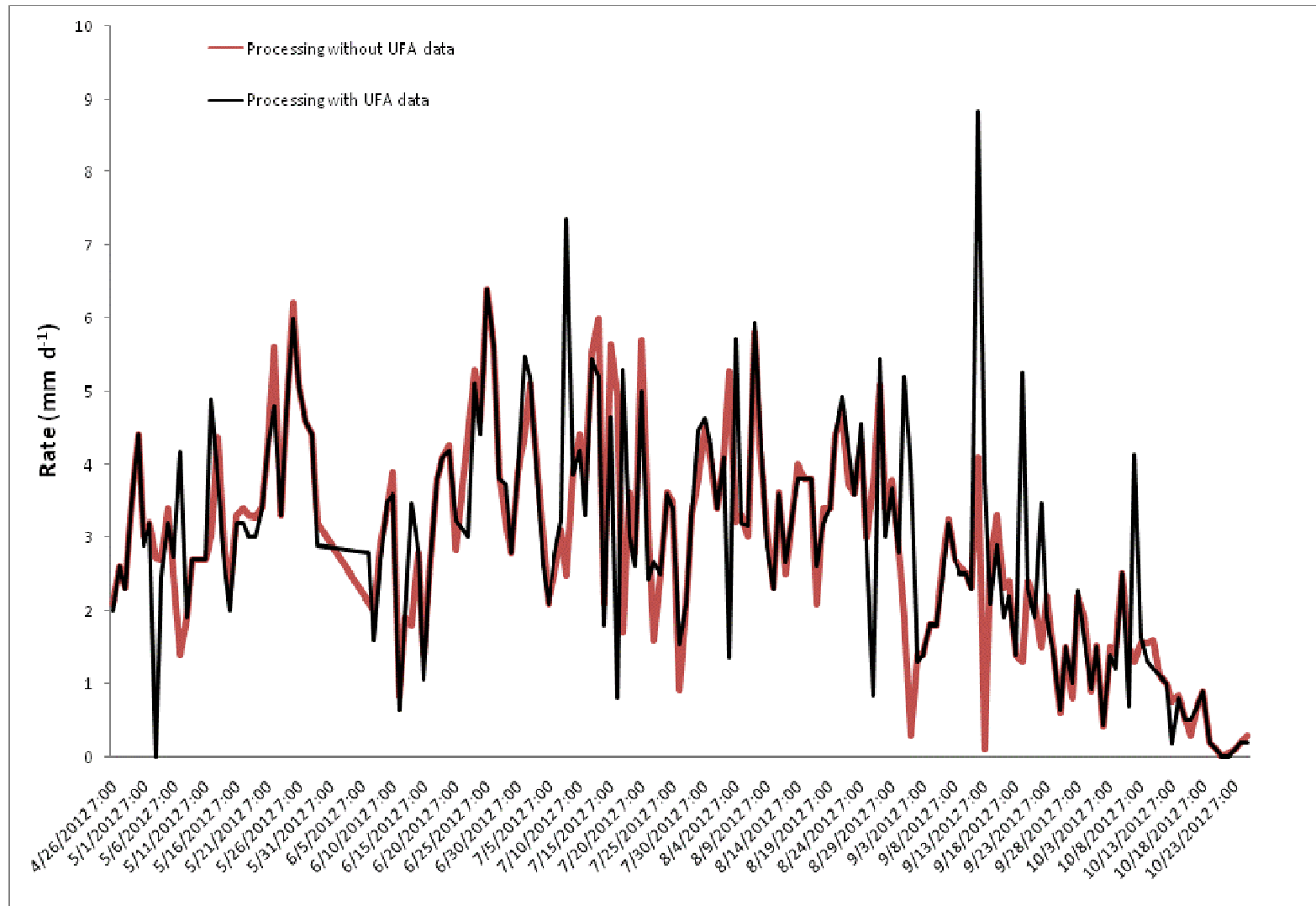
Appendix 6. Estimation of precipitation from EWM pan and UFA raingauge, year 2012



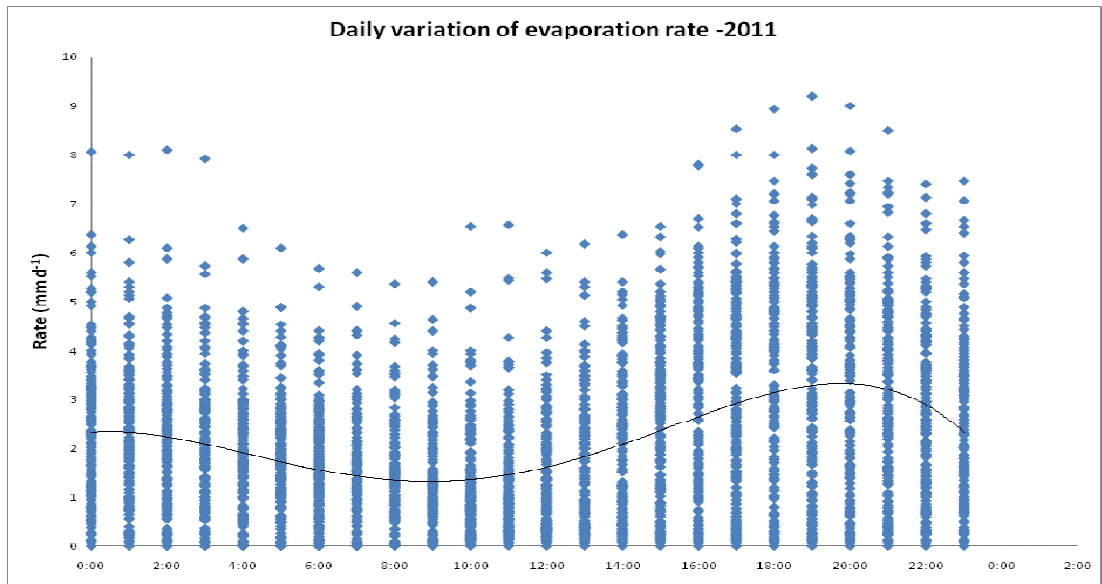
Appendix 7. Comparing net evaporation obtained from EWM pan with and without UFA raingauge, year 2011



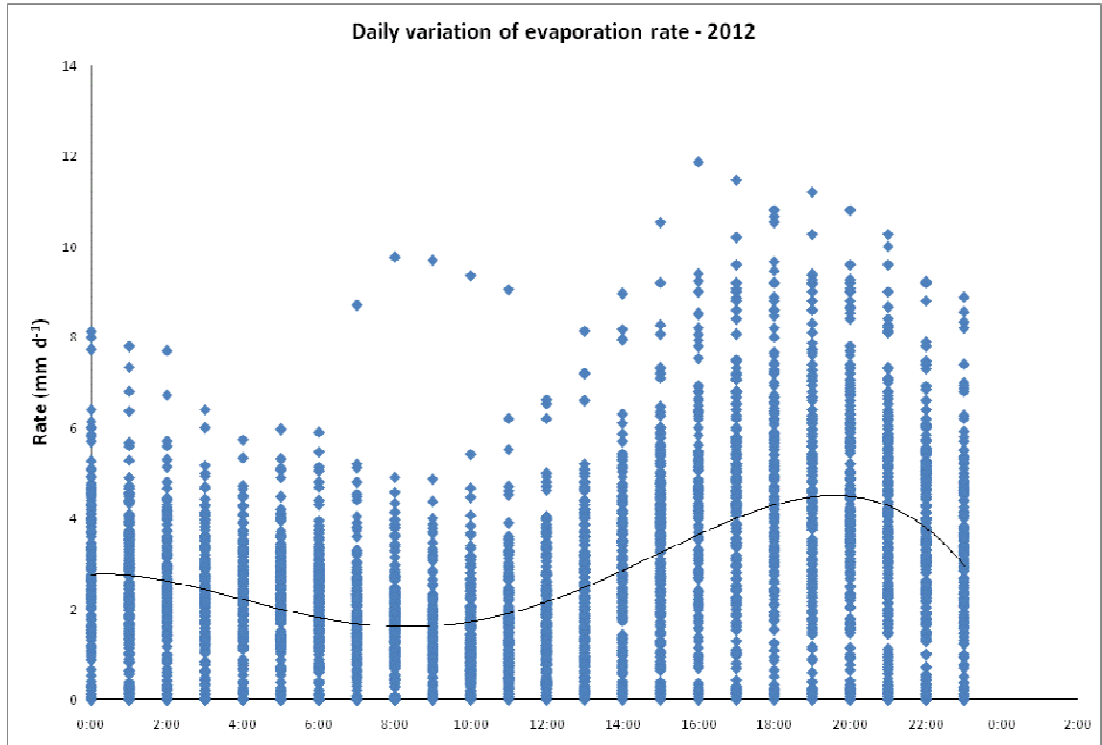
Appendix 8. Compare net evaporation obtained from EWM pan with and without UFA raingauge, year 2012



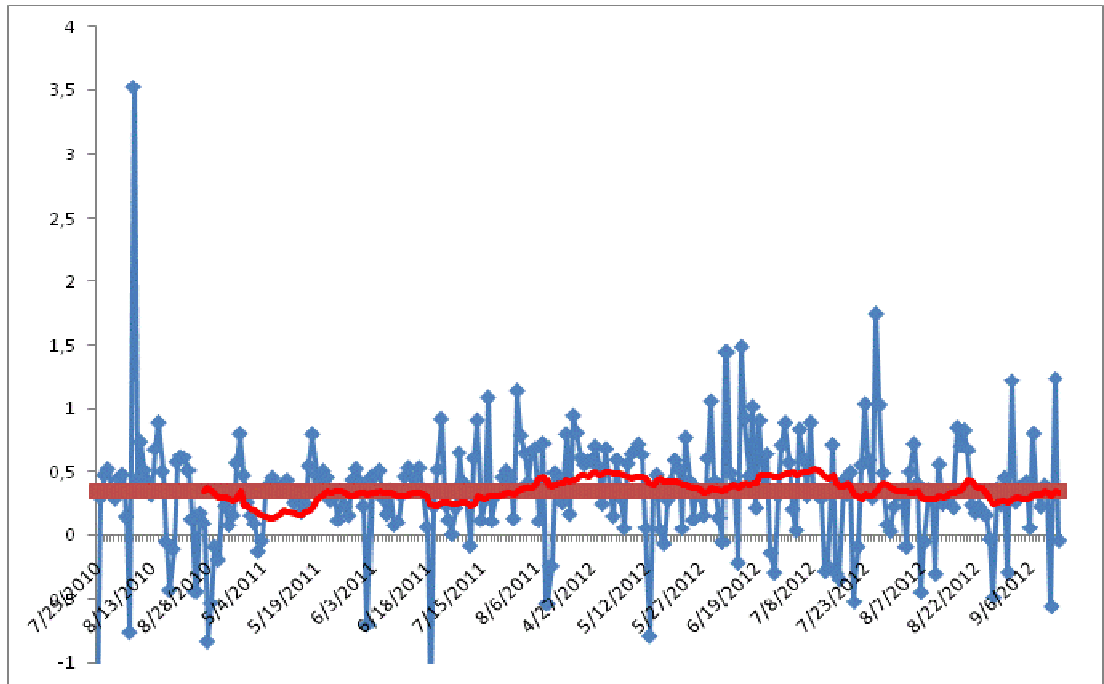
Appendix 9: Daily variation of evaporation rate - 2011



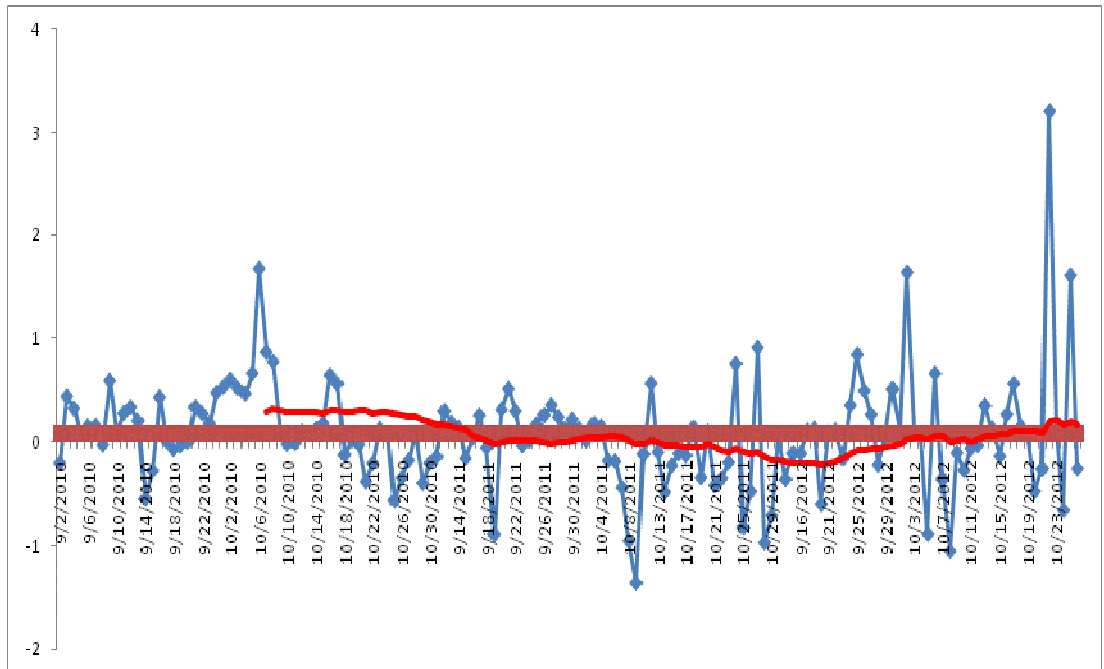
Appendix 10: Daily variation of evaporation rate - 2012



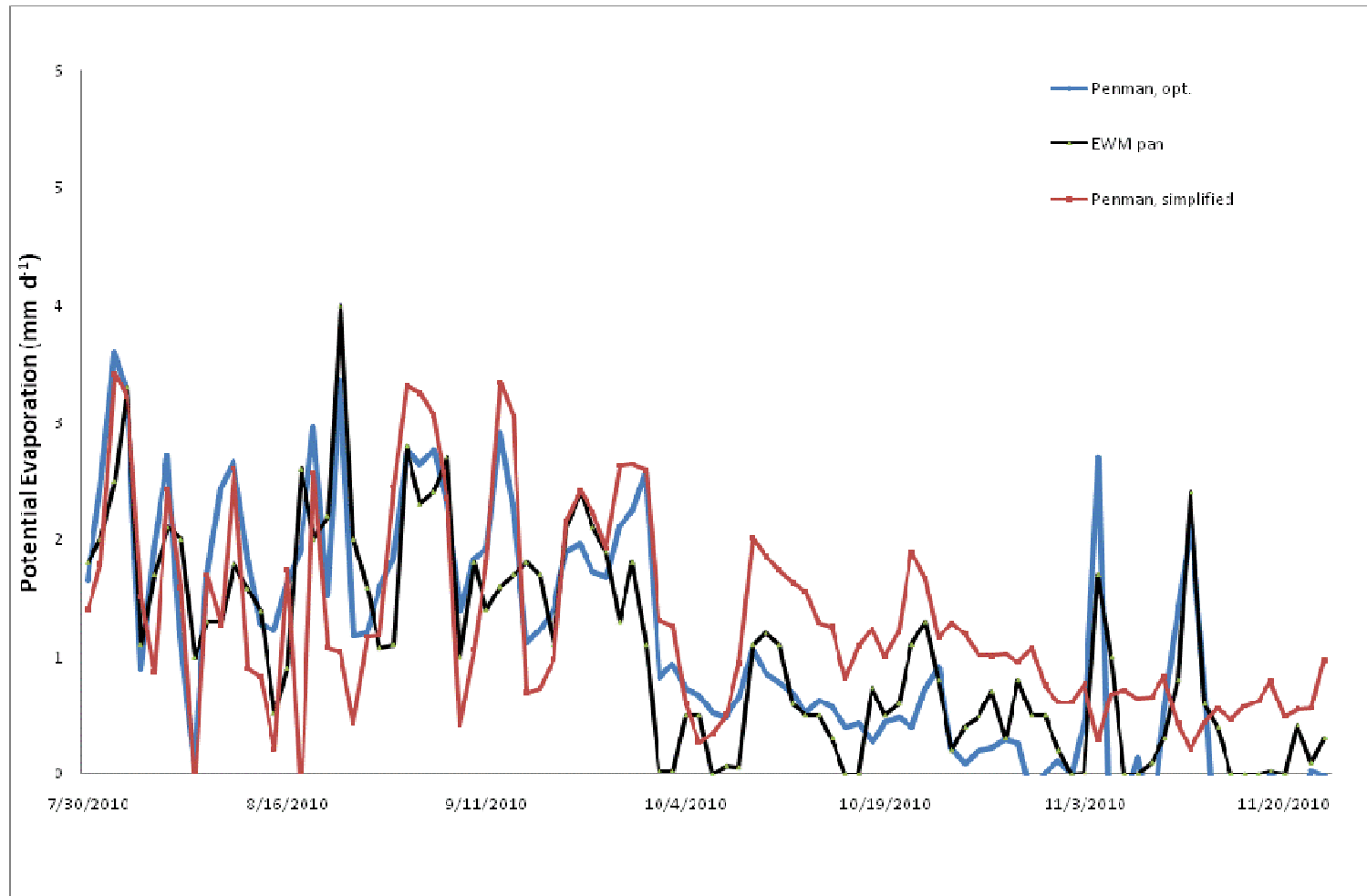
Appendix 11: Optimization of albedo for EWM pan water in summer time



Appendix 12: Optimization of albedo for EWM pan water in autumn time



Appendix 13: Net evaporation from EWM pan, Penman equation and the simplified form – 2010



Appendix 14 Net evaporation from EWM pan, Penman equation and the simplified form – 2012

